Limnology (2022) 23:17–35
https://doi.org/10.1007/s10201-021-00669-9

RESEARCH PAPER

Spatial–temporal heterogeneity in a small lake and its implication for paleoclimate reconstruction

Suman Rawat[1] · Anil K. Gupta[2] · Priyeshu Srivastava[3] · S. J. Sangode[4] · Luigi Jovane[3]

Received: 2 October 2020 / Accepted: 10 July 2021 / Published online: 23 July 2021

Abstract

Lakes provide continuous records of past regional and global climate. Most studies utilize single trench section dig from the lake shore margins or from single core in the central part/depocenter of the lakes for paleoclimate reconstruction. These reconstructions are based on the assumption of homogenous sedimentation across the lake. However, single core approach for paleoclimate reconstruction is often debated due to inter-site spatial and temporal variations in sedimentation and proxy responses. Therefore, in the present study, we explored the spatial–temporal heterogeneity in a small post-glacial lake of the Lahaul Himalaya and its influence on paleoclimate reconstruction. The depocenter of lake received ~ 2.5 times higher average sedimentation compared to the shore margin. Despite the distinct sedimentation rate in depocenter and shore margin, environmental magnetic and total organic carbon (TOC) records showed similar environmental signals over equivalent time periods. The depocenter core provided high-resolution lacustrine environment, whereas the marginal trench recorded major shifts in paleoclimate over a longer time scale. New multi-proxy data showed strengthened Indian summer monsoon (ISM) during medieval climate anomaly (MCA) and weakened ISM during little ice age (LIA) in the NW Himalaya.

Keywords Spatial heterogeneity · Paleolimnology · Paleoclimate · Indian summer monsoon · Himalaya

Introduction

Lake sediments are important environmental archive and continuous sedimentation provides an opportunity to study high-resolution paleoclimate variability of several millennia (e.g. Gasse et al. 1996; Williamson et al. 1998; Hodell et al. 1999; Kirby et al. 2004; Wünnemann et al. 2010; Rawat et al. 2015a, b; Rawat et al. 2021a). To retrieve the paleoenvironmental information from lacustrine sediments, several organic (e.g. total organic carbon, total nitrogen, stable isotopes of carbon and nitrogen, lipid biomarkers, pollen and diatoms) and inorganic (e.g. major and trace element geochemistry, grain size, stable oxygen isotopes, mineralogy and environmental magnetism) proxies are commonly applied. The paleoenvironmental studies from the lacustrine sediments are mostly based on single core considering that sedimentation is homogenous across the lake (e.g. Charles et al. 1991; Petterson et al. 1993; Fedotov et al. 2008; Finsinger et al. 2008; Lu et al. 2010). The single core approach has been suggested to be more valid for the small varved lakes compared to larger lakes owing to spatial consistency in the geochemical proxies (e.g. TOC, stable carbon and nitrogen isotopes) at annual scale (Gälman et al. 2008, 2009). Several studies reported spatial variability in sedimentations in non-varved lakes (e.g. Anderson 1990; Hilton et al. 1986; Fritz et al. 2006; Schiefer 2006). Organic geochemical proxies (e.g. lipid biomarker) have shown significant spatial heterogeneity in surface sediments of lakes and the core sediments from central part of the lake have been suggested to best represent the average variability (Sarkar et al. 2014). Along with this line of interpretation, Wang et al. (2009) had also suggested that single core from the deepest site can provide information about the total lake

Handling Editor: Jorge García Molinos.

✉ Suman Rawat
rsuman26@gmail.com

[1] Wadia Institute of Himalayan Geology, 33 G.M.S. Road, Dehradun 248 001, India

[2] Department of Geology and Geophysics, Indian Institute of Technology, Kharagpur 721302, India

[3] Instituto Oceanográfico, Universidade de São Paulo, Praça do Oceanográfico, 191, São Paulo 05508-120, Brazil

[4] Department of Geology, Savitribai Phule Pune University, Pune 411 007, India

environment, whereas cores from a shallow site may divulge shifts in environment over a longer time period.

A great number of studies on lacustrine sediments are being carried out from the Indian subcontinent to reconstruct the past Indian summer monsoon (ISM) precipitation (Misra et al. 2019). Most of these studies are based on the single core/trench approach either from the central part or from the marginal/shallower sites of the lake. The past ISM reconstruction is not only important to understand the changes in the socio-economic development of ancient Indian civilizations but also to contemporary and future climatic changes (Pokharia et al. 2017, 2020; Dixit et al. 2018; Dutt et al. 2018; Rawat et al. 2021a). Therefore, in this regard, we aim to understand the spatial–temporal heterogeneity in a small post-glacial lake (~60 m diameter) from the Chandra valley, Lahaul Himalaya and its impact on the paleoclimatic reconstruction (Fig. 1a, b). The lake has developed on the glacially sculpted bedrock (Fig. 1c). The water input in this lake is limited to snowmelt and rainfall over the restricted catchment (Rawat et al. 2015b). Therefore, the lake has a low sediment supply from a known catchment, which makes it an ideal site to evaluate the spatial and temporal variations in inorganic and organic proxies.

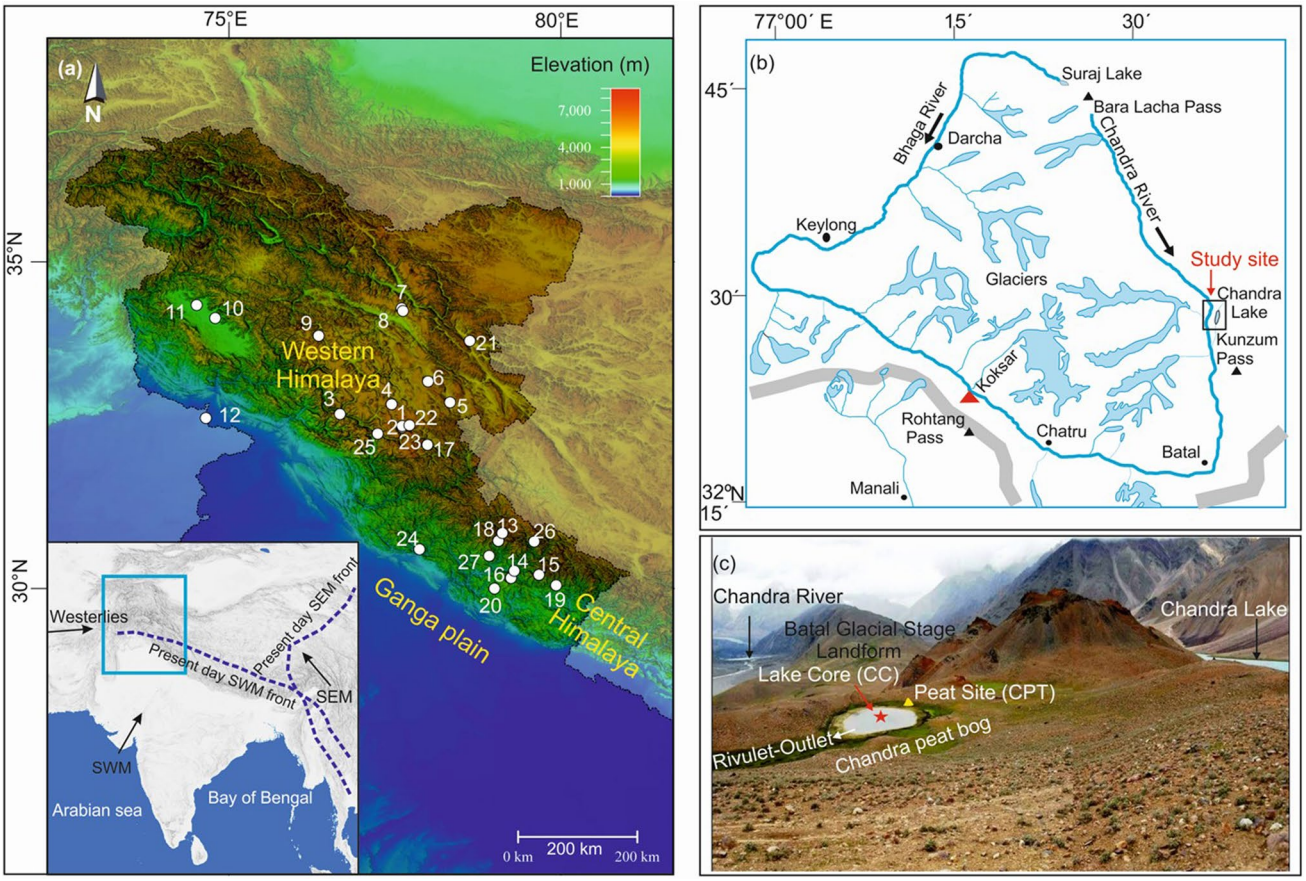

Fig. 1 **a** Map of the study area with different Asian monsoonal settings shown in the inset map. The white circles show location of studies in the NW and central Himalaya that have been discussed for the regional/local paleoclimate correlation. (1) Chandra post-glacial lake (Present study and Rawat et al. 2015a, b); (2) Chandra lake, Lahaul (Kumar et al. 2020; Shamurailatpam et al. 2020); (3) Triloknath Paleolake, Lahaul (Bali et al. 2017); (4) Yunam basin, Lahaul (Bohra and Kotlia 2015); (5) Tso Moriri, Ladakh (Leipe et al. 2014; Mishra et al. 2015a, b; Dutt et al. 2018); (6) Tso kar, Ladakh (Demske et al. 2009; Wünnemann et al. 2010); (7) North Pullu, Ladakh (Phartiyal et al. 2020); (8) South Pullu, Ladakh (Phartiyal et al. 2021); (9) Penzi-la pass, Zanskar valley (Ali et al. 2020); (10) Anchar Lake, Kashmir (Lone et al. 2020); (11) Wular Lake, Kashmir (Shah et al. 2020); (12) Gharana Wetland, Jammu (Quamar 2019); (13) Kedarnath, Alaknanda (Srivastava et al. 2017a, b); (14) Benital, Pinder (Bhushan et al. 2018); (15) Bedni, Pinder (Rawat et al. 2021a); (16) Badanital Lake, Rudraprayag (Kotlia and Joshi 2013); (17) Takche lake, Spiti (Mazari et al. 1995); (18) Bhujbasa, Gangotri (Kar et al. 2002); (19) Pinder valley (Phadtare 2000; Rühland et al. 2006); (20) Dewar Tal, Chamoli (Chauhan and Sharma 2000); (21) Pangong, Ladakh (Srivastava et al. 2020); (22) Sitikher bog, Spiti (Chauhan et al. 2000); (23) Naychhudwari bog, Parvati valley (Chauhan 2006); (24) Sahiya Cave (Kathayat et al. 2017); (25) Rohtang Pass (Bhattacharya 1988); (26) Tipra Bank Glacier (Bhattacharya and Chauhan 1997) and (27) Sainji Cave (Kotlia et al. 2015). **b** Map of the Chandra valley showing present study site (rectangle) with different glacier settings in the region. **c** Field photograph of the lake showing sampling site of the Chandra core (CC) and marginal shore Chandra peat trench (CPT) site. Figure is modified after Rawat et al. (2015a)

Previously, we had established paleoclimate from this region using multi-proxy data (i.e. pollen, stable carbon isotope, total organic carbon and environmental magnetism) from a marginal trench site [Chandra peat trench (CPT) sequence] of this lake (Fig. 1c) (Rawat et al. 2012, 2015a, b). For the present study, we collected a ~ 111 cm long core from the central/depocenter part of the same lake using a Russian Corer (Fig. 1c). The core samples were studied using environmental magnetism and total organic carbon proxies for spatial–temporal heterogeneity. We also analyzed major and trace element concentrations of lake core sediments for the paleoclimate reconstruction.

Study area and sample collection

The Lahaul Himalaya (~ 3500–5000 m a.s.l.) lies in the rain shadow zone due to the upliftment of Pir Panjal ranges during the Pleistocene creating an orographic barrier for moisture-laden winds of the ISM (Burbank 1982; Owen et al. 2001). This upliftment divided two climatic subdivisions of the NW Himalaya (1) high precipitation front on southern slopes of the Lesser Himalaya and (2) cold-dry semi-arid regions of the northern Trans-Himalaya i.e. Lahaul, Zanskar and Ladakh (Burbank 1982; Owen et al. 2001). The semi-arid regions receive precipitation from both ISM and mid-latitude westerlies bringing moisture from the Mediterranean regions (Fig. 1). The post-glacial small lake was developed on the glacially sculpted bedrock from Batal glacial stage (~ 15.5–12 ka) in the Chandra valley, Lahaul Himalaya (Fig. 1c). The Chandra core (CC) was carried out in the depocenter of the lake using a Russian corer and a ~ 111 cm long core was recovered (Fig. 1c). A total of 111 samples were collected by slicing the sediment core at every ~ 1 cm interval for high-resolution systematic magnetic, geochemistry and TOC analyses. The detailed lithological description of the core is given in Supplementary Figure S1. The rocks in the study area are composed of sedimentary succession of the Kunzam La Formation of the Haimanta Group overlying on the crystalline rocks of the Vaikrita Group. The Kunzam La Formation is comprised of siltstone, shale, slate, quartzite, sandstone and limestone/dolomite. The Kunzam La Formation rocks are of the Cambrian age (Bhargava et al. 1991; Srikantia and Bhargava 2018) and were deposited in a deep to shallow shelf setting in a low-energy depositional environment (Parcha and Pandey 2016).

Methodology

AMS ^{14}C chronology

Three AMS ^{14}C dates on bulk organic sediments at different depth intervals of the lake core was analyzed at National Ocean Sciences Accelerator Mass Spectrometry (NOSAMS) facility of the Woods Hole Oceanographic Institution (MA, USA). A detailed description of the sample treatment, processing and method of AMS ^{14}C dating can be accessed from https://www.whoi.edu/nosams/home. The calibration of AMS ^{14}C ages (using IntCal13 data set) and construction of the age-depth model was carried out using the Bacon package (version 2.3.9.1) in R software (version 3.4.2) (Blaauw and Christen 2011; Reimer et al. 2013).

Environmental magnetism

The low- and high-frequency magnetic susceptibilities (χ_{lf} = 0.46 kHz and χ_{hf} = 4.65 kHz, respectively) were measured using a Bartington MS2B laboratory sensor. The frequency-dependent susceptibility $\chi_{fd} = (\chi_{lf} - \chi_{hf})$ and corresponding percentage frequency-dependent susceptibility $\chi_{fd}\% = [(\chi_{lf} - \chi_{hf})/\chi_{lf} \times 100]$ were calculated. Anhysteretic remanent magnetization (ARM) was imparted at the alternating field of 100 mT peak field superimposed over 0.1 mT DC field using a Molspin AF Demagnetizer and remanence was measured using a Minispin Fluxgate Spinner Magnetometer. ARM was normalized by DC bias field strength and divided with the density to acquire the susceptibility of anhysteretic remanent magnetization (χ_{ARM}). Saturation isothermal remanent magnetization (SIRM) was induced at 1000 mT forward field. Backfield IRM (BIRM) was measured at − 300 mT for calculation of parameters hard isothermal remanent magnetization (HIRM = 0.5 × (SIRM + IRM_{-300mT})) and S-ratio (− IRM_{-300mT}/SIRM). SIRM and BIRM were induced using an ASC Model IM-10-30 Impulse Magnetizer and remanences were measured using a Minispin Fluxgate Spinner Magnetometer. Magnetic susceptibility, ARM, SIRM and BIRM were measured at Paleomagnetic Laboratory, Wadia Institute of Himalayan Geology (WIHG) and at Department of Geology, Savitribai Phule Pune University, India.

For detailed magnetic mineralogy, selected samples were analyzed for hysteresis loop and IRM acquisition at progressively higher DC fields up to a maximum field of 1 T in 150 steps using a Princeton Measurements Corporation Model 3900 Micromag Vibrating Sample Magnetometer. Saturation magnetization (Ms), saturation remanence (Mrs) and coercive force (Hc) were calculated from the slope (paramagnetic) corrected hysteresis loops. The coercivity of remanence (Hcr) was calculated from back-field remanence curves. The un-mixing of magnetic coercivity distributions from IRM acquisition data was performed using the web application MAX UnMix (Maxbauer et al. 2016). Temperature dependence of the magnetic susceptibility was measured up to a maximum temperature of 700 °C in an argon atmosphere using a furnace-equipped KLY-4 (AGICO) Kappabridge. Hysteresis loop, IRM acquisition curves and

temperature dependence of the magnetic susceptibility measurements were performed at Centro Estratigráfico de Registros Oceanográfico (CORE), Instituto Oceanográfico, Universidade de São Paulo, Brazil.

Total organic carbon (TOC)

For TOC analysis, fine powdered sediment samples were first treated with 0.6 N HCl to remove inorganic carbonate contents. Then, ~ 0.2 to 20 mg of carbonate free powered samples were packed into the tin capsule and combusted at ~ 1020 °C in an oxygenated environment in Flow Isotope Ratio Mass Spectrometer (CFIRMS) coupled with Flash Elemental Analyzer (EA) at WIHG. TOC was calculated from peak areas obtained from the sum of integrated m/z 44, 45 and 46 signals measured in the CFIRMS.

Elemental geochemistry

Major and trace element concentrations of the lake core sediment samples were determined by solution method using a PerkinElmer Elan-DRCe inductively coupled plasma mass spectrometer (ICPMS) at WIHG. A 100 mg fine powdered sample was digested with 10 ml of AR grade HF-HNO_3 mixture (2:1) in open Teflon (PTFE) crucibles on a hot plate. The process was repeated 3–4 times for complete digestion. This was followed by two treatments with 2 ml AR grade $HClO_4$ and further evaporation to complete dryness. The dried mass was then dissolved in 10 ml of 20% HNO_3 and the final volume was made up to 100 ml using distilled water. The sediment standard MAG-1 and shale standard SGR-1 were digested under similar conditions for calibration. A batch of ten samples, a blank and two standards (MAG-1 and SGR-1) were made and measured. The accuracy and precision of analysis for various major and trace elements were achieved between 1 and 10% and 1–9% RSD, respectively.

Statistical analysis

We calculated Pearson's correlation coefficients and performed Principal Component Analysis (PCA) analysis on all data of major and trace elements, TOC and environmental magnetic parameters of the Chandra core. These analyses were performed using the data analysis tool package in excel program and Origin software.

Results and interpretations

AMS ^{14}C chronology

The result of AMS ^{14}C chronology of the CC samples is provided in Table 1. The base sample at ~ 111–110 cm depth of the core produced an age of ~ 5514 cal years BP. The ages of individual sediment depth horizons at each cm interval were based on interpolated weighted median age calculated from Bacon analysis (Supplementary Table S1). The Bacon age-depth model result of the CC profile is presented in Fig. 2a. Sediment accumulation rate (SAR) of the CC profile varied from ~ 0.07 to 0.63 mm year^{-1} (Fig. 3a). Four distinct sediment accumulation phases were identified in the CC sediments (Fig. 3a). (1) Low sedimentation: ~ 0.09 mm year^{-1} (avg.) from ~ 5514 to 2178 cal years BP; (2) medium sedimentation: ~ 0.26 mm year^{-1} (avg.) from ~ 2178 to 1900 cal years BP; (3) high sedimentation: ~ 0.5 mm year^{-1} (avg.) from ~ 1900 to 980 cal years BP, and (4) medium sedimentation: ~ 0.3 mm year^{-1} (avg.) from ~ 980 cal years BP to Present (Fig. 3a).

Magnetic mineralogy and concentration

The magnetic concentration parameters [(χ_{lf} = ~ 1.8–23.1 ($\times 10^{-9}$m^3 kg^{-1}); SIRM = ~ 6.3–164.3 ($\times 10^{-5}$A m^2 kg^{-1}) and χ_{ARM} = 0.63–92.5 ($\times 10^{-8}$m^2 kg^{-1})] showed highly variable distribution of magnetic minerals throughout the core profile (Supplementary Table S2; Fig. 4). χ_{fd}% and χ_{fd} varied from 0 to 17% and 0–1.70 ($\times 10^{-9}$m^3 kg^{-1}), respectively, indicating a total absence of superparamagnetic (SP) ferrimagnetic particles to their low presence in lake sediments. χ_{fd}% > 5 was found only in top lake sediment sequence (past ~ 1200 years) indicating presence of SP ferrimagnetic particles in recent sediments. S-ratio varied between 0.30 and 1 indicating variations from antiferromagnetic (e.g. hematite) rich sediments to ferrimagnetic (e.g. titanomagnetite) rich sediments in the lake core samples (Supplementary Table S2; Fig. 4).

Table 1 The AMS ^{14}C radiocarbon ages of the Chandra Core

Sample Id	Depth (cm)	Lab no	Sample type	AMS ^{14}C ages (years BP)	Minimum age (cal years BP)	Maximum age (cal years BP)	Median age (cal years BP)
CC-29	28–29	OS-98755	Bulk organic sediments	1050 ± 45	768	1051	933
CC-77	76–77	OS-98754	Bulk organic sediments	1960 ± 35	1819	2304	1938
CC-111	110–111	OS-98751	Bulk organic sediments	4830 ± 50	5236	5701	5514

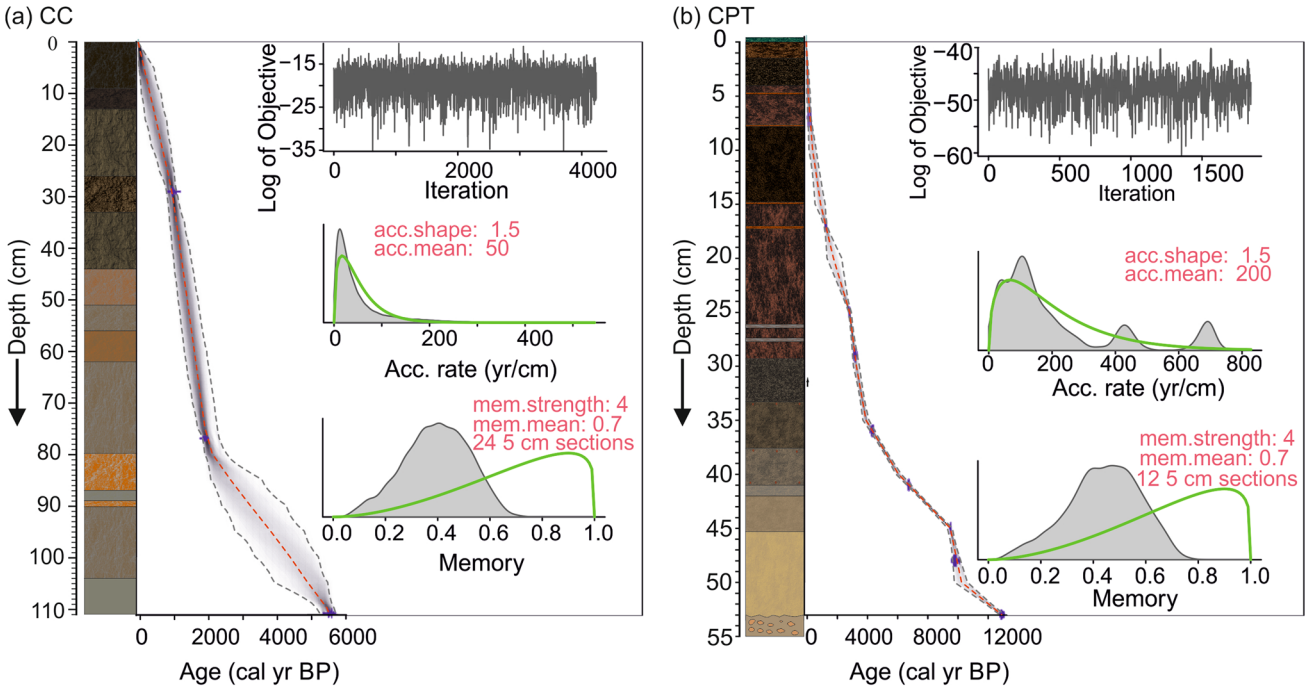

Fig. 2 Bacon age-depth models of **a** the depocenter core CC and, **b** the shore CPT profiles. The calibrated ages are shown in blue. The dotted lines (grey) indicate the 95% confidence limits and the dashed line (red) shows the weighted median ages for each depth. The age data of CPT profile is after Rawat et al. (2015a)

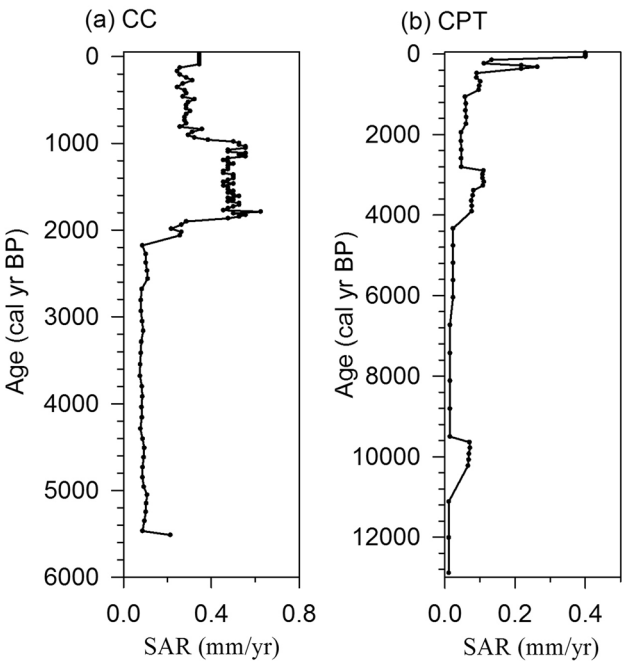

Fig. 3 Sedimentation rate (mm year^{-1}) plotted against calibrated ages of **a** CC profile and, **b** CPT profile

Hysteresis loop and its parameters (Ms, Mrs, Hc and Hcr) are diagnostic for understanding magnetic mineralogy and grain size/magnetic domains (Dunlop 2002). Hysteresis results for all selected samples from different depth intervals showed similar shapes with loops closing below 300 mT and there was no signature of wasp-waisted feature indicating dominant unimodal population of low coercivity ferrimagnetic minerals (Fig. 5a–e). Hc and Hcr varied from ~ 21.9 to 32.7 mT and ~ 44.1–52.1 mT, respectively, indicating typical characteristics of fine pseudo single domain magnetite or mixed multidomain and pseudo single domain magnetite (Roberts et al. 1995; Peters and Dekkers 2003) (Fig. 5a–e).

The IRM un-mixing results showed three distinct magnetic components (Fig. 5f–j). The model results output are given in Supplementary Table S3. The low component (component 1) had mean coercivity (Bh) for all samples between 1.33 and 1.50 $\log_{10}$ units (21.5 to 31.6 mT) and dispersion (DP) between 0.27 and 0.38 broadly suggesting that this low coercivity ferrimagnetic component is possibly pedogenic magnetite (Maxbauer et al. 2016). The medium coercivity component (component 2) Bh ranged between 1.87 and 1.95 $\log_{10}$ units (74.7–89.2 mT) and DP between 0.26 and 0.31. This medium coercivity component 2 possibly indicated partially oxidized/altered single domain (SD) magnetite or maghemite and had the highest proportions in all the samples. The high coercivity component (component 3) had Bh range from 2.58 to 2.83 $\log_{10}$ units (~ 382 to 676.4 mT) and DP between 0.25 and 0.45. This high coercivity component 3 showed the presence of hematite.

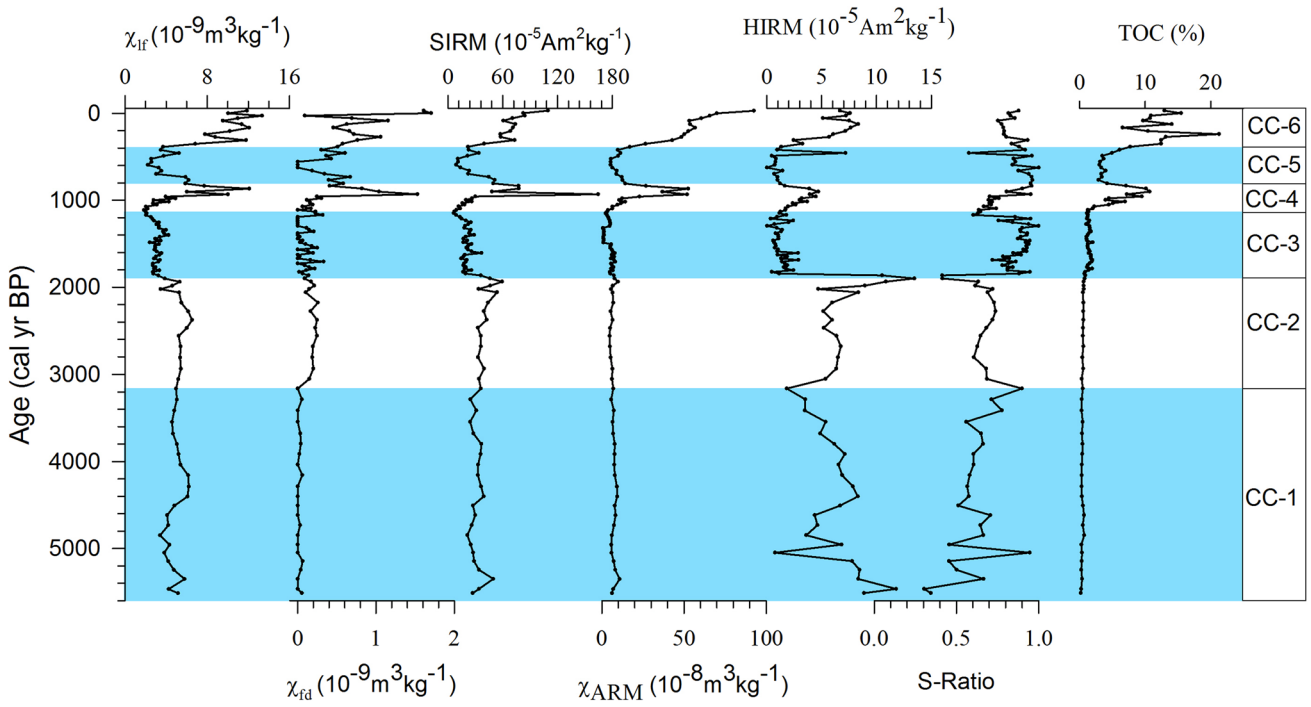

Fig. 4 Environmental magnetic parameters and total organic carbon plotted against calibrated ages of the CC profile

The temperature-dependent magnetic susceptibility showed similar behavior for all the analyzed samples with two increases in magnetic susceptibility i.e. (1) minor increase in susceptibility starting at ~ 250 °C with peak susceptibility around 290 to 300 °C, and (2) major increase in susceptibility starting at ~ 420 °C with peak susceptibility around ~ 490 to 500 °C followed by complete loss of magnetization between ~ 570 and 590 °C (Fig. 5k–o). The minor increase in susceptibility at ~ 250 °C with peak around ~ 290–300 °C indicated the transformation of weakly magnetic minerals such as ferrihydrite to relatively stronger magnetic minerals such as maghemite (Hanesch et al. 2006). The major increase in susceptibility starting at ~ 420 °C with peak susceptibility at ~ 490–500 °C was possibly due to either thermochemical alteration of paramagnetic clays and/or pyrite into magnetite, which was identified by the Curie temperature of ~ 570 to 590 °C (Jovane et al. 2019) (Fig. 5k–o). The other possibility of this increase was from either goethite or hematite transformation into magnetite under reducing environment created by the decomposition of organic matter present in samples and release of CO_2 (Hanesch et al. 2006; Dekkers 1990; Jordanova and Jordanova 2016). The IRM unmixing results showed presence of antiferromagnetic mineral hematite in all samples with low proportions as well as organic carbon from TOC measurements. Varying amount of organic carbon and paramagnetic clays may have control on the neoformed minerals and their concentration which can be seen from variable increase in susceptibility of cooling curves.

Geochemistry and total organic carbon

The concentration data of 24 major and trace elements and TOC analyzed for all 111 samples of the Chandra core are provided in Supplementary Table S4. The TOC data varied between 0.20 and 21.24% indicating the highly variable distribution of organic matter implying significant changes in the paleo-productivity of lake in response to changing climate/precipitation. The PCA analysis showed four principal components with eigenvalues > 1 amounting to 77.85% of the cumulative variance (Supplementary Table S5). The maximum variance was shown by PC1 with 58.48% followed by PC2 representing 10.20% of the total variance. Most of the major and trace elements, magnetic concentration parameters and organic carbon data (Ti, Ca, Mg, Mn, P, Sr, V, Co, Cr, Zn, Cd, Pb, Sc, Li, U, χ_{lf}, χ_{fd}, SIRM, χ_{ARM} and TOC) were strongly loaded on the PC1. Fe, Ba, Rb, Ni, Cu, Th and HIRM were moderately loaded on PC2 (Supplementary Table S5). Al, Na and K were strongly loaded on the PC3 which amount to 5.04% of total variability. Biplot with loadings and the scores for PC1 and PC2 is shown in Supplementary Figure S2. Except K, most parameters showed a positive correlation (Supplementary Figure S2). The PCA tool has been useful in distinguishing the changes in redox conditions in the lake environment during different

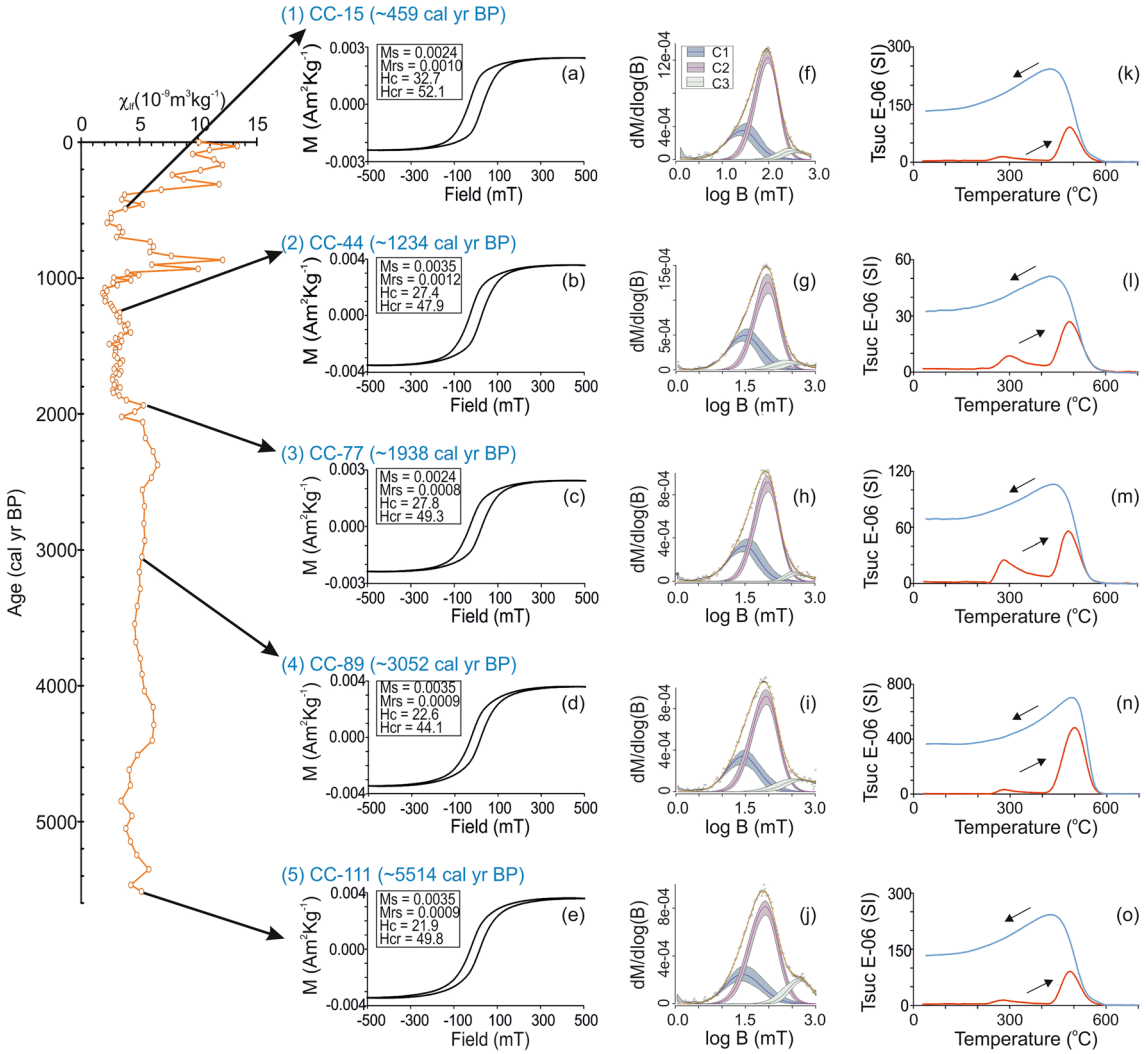

Fig. 5 Rock magnetic results on the selected samples of the CC profile. **a–e** Hysteresis plots; **f–j** IRM Un-mixing and **k–o** temperature-dependent magnetic susceptibility

time intervals (e.g. Garnier et al. 2020). In present analysis, a distinguished segregation or clustering between redox sensitive and terrigenous proxy was not clearly observed. However, organic proxies (TOC and P) showed a distinct clustering than terrigenous proxies (e.g. Al and Ti) (Supplementary Figure S2). Further, based on strong and moderate loadings of most of the data on PC1, it could not be specifically assigned to a single process but to a number of processes that might work in close association in a lake system e.g. detrital input, oxidation–reduction and organic processes (Supplementary Table S5).

The Pearson's correlation coefficient for most of the analyzed major and trace elements showed moderate ($r=0.50$–0.70) and strong ($r=0.70$–0.99) positive correlations amongst themselves and such correlations are commonly expected in catchment weathering and lakes depositional systems e.g. Fe showed moderate positive correlation with Ti and strong correlation with trace metals Ni, Cu, Co and Zn (Supplementary Table S6). These trace elements are generally hosted in weathering resistant primary minerals (e.g. Fe–Ti oxides/titanomagnetite) and/or adsorbed on secondary Fe–Mn oxides and clays (e.g. Srivastava et al. 2018a). Magnetic susceptibility also showed moderate and strong positive correlations with Fe, Ti, Mn, V, Cr, Ni, Co, Zn, Pb, Cd, Li and U (Supplementary Table S6). Mn and Mg showed strong correlations amongst themselves and with other trace elements e.g. V, Ni, Co, Sc, Zn, U and Th (Supplementary Table S6). Generally, Mg is retained in weathering system owing to its high compatibility with clays, whereas secondary Fe–Mn oxides are formed from alteration of primary minerals (Srivastava et al. 2018a). These trace elements (V, Ni, Co, Sc, Zn, U and Th) are adsorbed on clays and Fe–Mn oxides depending on the redox conditions. Organic matter has been also suggested to have the adsorption capability of

trace elements (Sharma et al. 2004). Positive correlations amongst TOC and trace elements were found (Supplementary Table S6). P in lake sediments functions as an important nutrient for lake productivity and showed strong correlations with TOC (Supplementary Table S6).

Since precipitation is one of the dominant factors that control weathering of catchment rocks, lake sediments in monsoon-dominated areas are often evaluated for chemical weathering to understand the precipitation strengths during different time intervals. Chemical index of alteration (CIA) ($= 100 \times Al_2O_3/(Al_2O_3 + Na_2O + K_2O + CaO^*)$ is often employed to understand the in-situ weathering of rocks as more liable elements (e.g. Na, Ca and K) are more easily leached off from primary minerals, and residue weathered products gets enriched in Al-rich clays resulting in higher CIA values (Nesbitt and Young 1982; Fedo et al. 1995; Srivastava et al. 2018b). However, in closed lake basins, the reverse CIA values are used to indicate chemical weathering intensity i.e. high CIA values are referred to low chemical weathering. This is due to the fact that more liable elements/oxides (soluble) get deposited in lake basins and become enriched (Zhisheng et al. 2011; Minyuk et al. 2014; Liu et al. 2014). In present studied lake, a small rivulet outlet exists indicating that this lake is not an entirely closed lake and therefore, solute/soluble chemical elements (e.g. Na, Ca, Sr and K) are also expected to be partly lost from the lake thorough rivulet. However, some elements like Ca and Sr may be retained in the lake basin due to authigenic carbonate precipitation. Elements such as K, Rb, Mg and Ba are also easily leached off from primary minerals during chemical weathering but can be adsorbed by secondary clay minerals (Nesbitt et al. 1980; Nesbitt and Markovics 1997; Srivastava et al. 2018b) and, therefore, these elements become enriched in the weathering residue and only lost upon extreme chemical weathering (Nesbitt et al. 1980; Nesbitt and Markovics 1997). Al, Fe and Ti are conservative elements and with increasing chemical weathering processes they tend to be enriched in weathering products (Nesbitt et al. 1980; Condie et al, 1995; Nesbitt and Markovics 1997). As weathered residue products may compose the majority of the detrital components in open or partly open lake sediments, we employ CIA and ratios such as Al/Na, Al/Ca, Al/Mg, Al/Ti, Ti/Na and Li/Ba to understand the chemical weathering intensity during middle Holocene (Fig. 6). Higher values of these ratios indicate higher chemical weathering in catchment whereas low values indicate low chemical weathering. The CIA values ranged from 50.47 to 84.7 indicating unaltered/incipient to moderate chemical weathering of lake sediments (Supplementary Table S4; Fig. 6). The CIA accompanying ACNK plot showed moderate chemical weathering and follows the expected weathering trend of catchment rocks (Fig. 7).

The Rb/Sr is one of the most commonly used parameters applied in closed lake basin sediments to determine the chemical weathering intensity of catchment rocks due to their unique behavior (Jin et al. 2001). Rb is mostly incorporated in K-bearing silicates which are relatively more resistant to weathering compared to Na/Ca minerals or carbonate

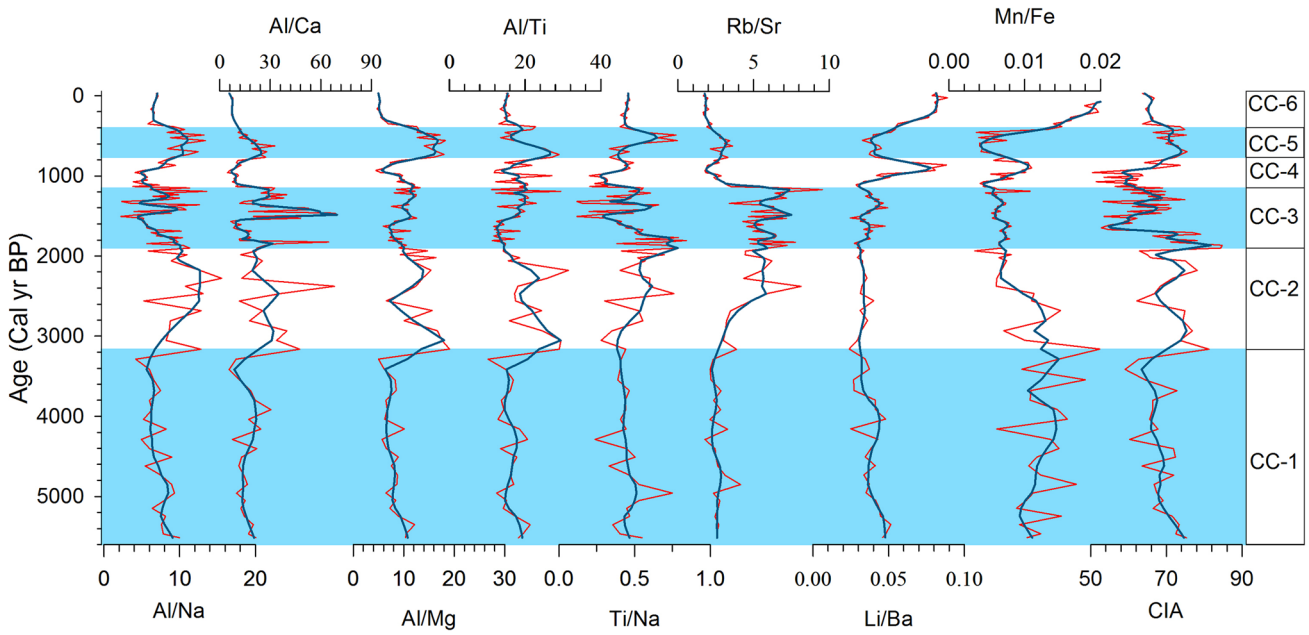

Fig. 6 Elemental ratios and chemical index of alteration (CIA) plotted against calibrated ages of the CC profile. The dark blue line overlain on the data represents LOESS Smoothing (factor = 0.06)

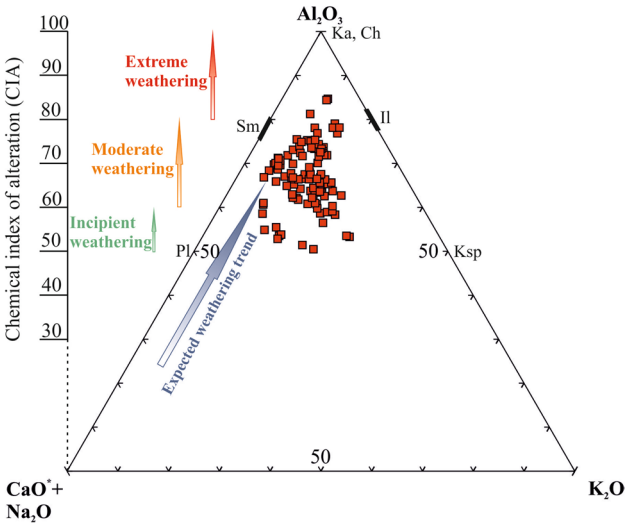

Fig. 7 Ternary plot of ACNK along with chemical index of alteration (CIA) of the CC samples

rocks of catchments (Jin et al. 2006; Chen et al. 1999). Further, upon higher chemical weathering, Rb can be retained in weathering residue in K-rich clays e.g. illite. While Sr behaves similarly to Ca in many geochemical processes substituting for Ca in minerals and is easily leached off into lake basins as dissolved Sr^{2+} load under enhanced chemical weathering (Jin et al. 2001, 2006). Therefore, weathering residue in catchment rocks becomes enriched in Rb/Sr whereas lake sediments have low Rb/Sr indicating higher chemical weathering. Often studies show that Rb/Sr ratio in lake sediments are mainly controlled by Sr activity by showing the strong negative correlation between Rb/Sr and Sr or a strong positive correlation with CIA (Jin et al. 2001, 2006; Zhisheng et al. 2011). The Rb/Sr showed strong negative correlation ($R^2 = 0.93$) with Sr, whereas, Rb/Sr did not show any correlation with CIA ($R^2 = 0.01$) (Fig. 8). In present studied lake sediments Rb (~ 80–159 ppm) also showed highly variable distribution along with Sr (~ 13–94 ppm) (Supplementary Table S4). Therefore, Rb/Sr in this lake setting indicates a more physical weathering dominant process than chemical weathering and therefore, high Rb/Sr may indicate higher physical weathering/erosion.

Chronology-wise variations in environmental magnetic, geochemistry and TOC data

The Chandra core record is divided into six zones primarily based on visual observations on gradual or sharp changes in environmental magnetic, geochemistry and TOC data.

CC Zone-1 (111–90 cm; ~ 5514 to 3160 cal years BP)

The magnetic concentration parameters χ_{lf}, SIRM and χ_{ARM} did not show any trend suggesting no significant changes in ferrimagnetic concentration in this period (Fig. 4). S-ratio ranged between 0.30 and 0.95 (average = 0.59) suggesting dominant antiferromagnetic mineral composition in this zone. HIRM, an indicator of antiferromagnetic mineral (e.g. hematite) concentration, showed a significant decreasing trend (Fig. 4). TOC ranged between 0.2 and 0.7% indicating an overall low concentration of organic matter (Fig. 4). Al/Na, Al/Mg and CIA showed a decreasing trend indicating lower chemical weathering intensity (Fig. 6). Mn/Fe showed relatively higher values between ~ 5500 and 2200 cal years BP. Ti/Na and Li/Ba did not show any significant trend in this zone (Fig. 6).

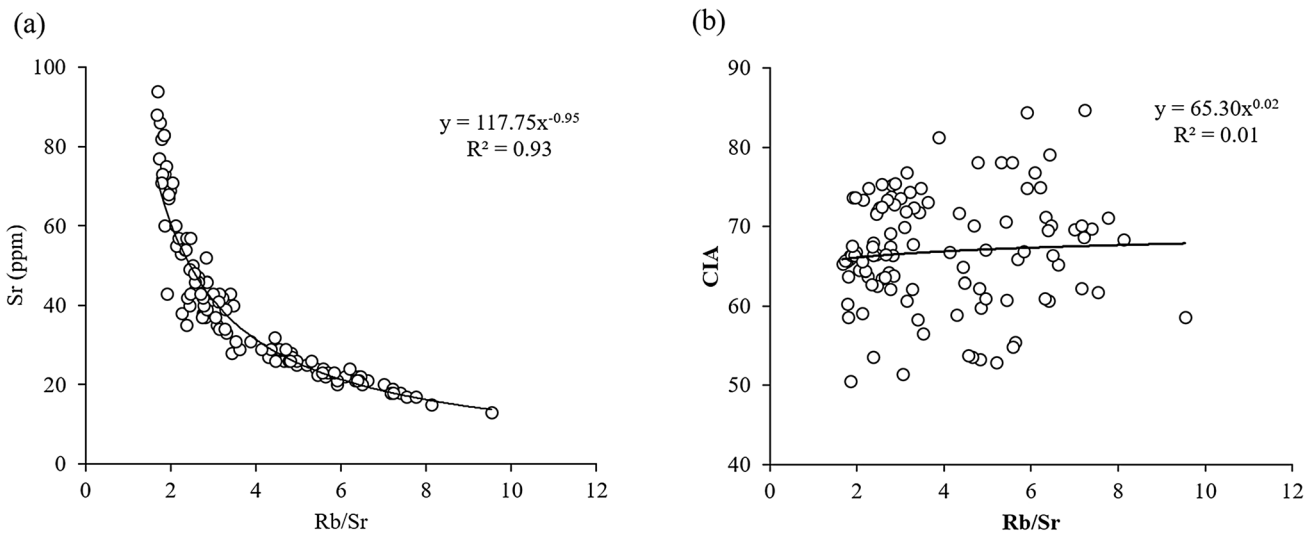

Fig. 8 Bivariate plots **a** Sr and Rb/Sr, and **b** CIA and Rb/Sr

CC Zone-2 (90–76 cm; ~ 3160 to 1900 cal years BP)

The minor increase in SIRM and χ_{lf} and significant increase in HIRM suggested an increased concentration of magnetic minerals (Fig. 4). S-ratio ranged from 0.41 to 0.90 (average = 0.61) indicating relative abundance of antiferromagnetic minerals. TOC varied between 0.4 and 0.8% indicating low organic carbon content (Fig. 4). Al/Na, Al/Ca, Al/Mg, Al/Ti, Ti/Na and CIA showed increased values in this zone indicating relatively higher chemical weathering (Fig. 6).

CC Zone-3 (76–40 cm; ~ 1900 to 1150 cal years BP)

A decrease in all magnetic concentration parameters indicated an overall decrease in bulk magnetic minerals concentration in this zone (Fig. 4). TOC ranged from 0.8 to 2% indicating low organic carbon content (Supplementary Table S4; Fig. 4). This zone showed highly fluctuating values with overall lower values of CIA, Al/Na and Ti/Na (Fig. 6). Interestingly, Rb/Sr showed significantly increased values in this zone (Fig. 6). This zone also showed maximum sedimentation implying that Rb/Sr coincides well with changes in sedimentation and validates a proxy for detrital/terrigenous input in these lake settings.

CC Zone-4 (40–24 cm; ~ 1150 to 770 cal years BP)

This zone was characterized by an increased concentration of magnetic minerals (Fig. 4). χ_{fd}% and χ_{fd} also showed the presence of SP ferrimagnetic particle in this zone (Supplementary Table S2; Fig. 4). TOC ranged from ~ 1.3 to 10.7% indicating significantly increased organic productivity during this period (Fig. 4). Li/Ba and Mn/Fe showed increased values, whereas Al/Na, Al/Ca, Al/Mg, Al/Ti, Ti/Na and CIA showed low/decreased values (Fig. 6).

CC Zone-5 (24–13 cm; ~ 770 to 390 cal years BP)

The low values of all the magnetic concentration parameters indicated decreased bulk magnetic concentration in this zone (Fig. 4). TOC showed significantly decreased values as compared to the previous zone (Fig. 4). Li/Ba and Mn/Fe have declined in this zone. Al/Na, Al/Ca, Al/Mg, Al/Ti, Ti/Na and CIA showed increased values (Fig. 6).

CC Zone-6 (13–0 cm; ~ 390 cal years BP to present)

All the magnetic concentration parameters showed an increasing trend in this zone indicating the increased concentration of bulk magnetic minerals (Fig. 4). TOC ranged from ~ 6.5 to 21.2% with an average of 12.5% suggesting maximum organic content in this zone (Supplementary Table S4; Fig. 4). Li/Ba and Mn/Fe have increased during this period. Al/Na, Al/Ca, Al/Mg, Al/Ti, Ti/Na and CIA showed a decreasing trend (Fig. 6).

Discussion

Spatial and temporal variations in marginal trench and depocenter core

For comparison of sedimentation rate in depocenter core (CC) and marginal trench (CPT; Rawat et al. 2015a) profiles, the AMS ^{14}C ages of the CPT profile were re-calibrated with the IntCal13 calibration data set using Bacon package (version 2.3.9.1) in R software (version 3.4.2) and age-depth model was developed (Supplementary Table S1; Fig. 2b). The SAR of the CPT profile is presented in Fig. 3b. The sedimentation in both shore margin and depocenter of the lake was continuous. The average SAR for the CPT profile was ~ 0.13 mm year^{-1} for past ~ 5600 years, whereas the average SAR for the CC profile was ~ 0.32 mm year^{-1} for past ~ 5500 years. This indicated that the depocenter of the lake had received ~ 2.5 times higher sedimentation compared to the shore margin site, which is in accordance with the several studies (e.g. Hilton et al. 1986; Wang et al. 2009).

The spatial and temporal correlations of data using graphical/stratigraphy observation for environmental magnetic (χ_{lf} and HIRM) and organic proxies (TOC) from marginal CPT and depocenter CC profiles are provided in Fig. 9. χ_{lf} and HIRM data of both CC and CPT profiles showed a good correlation (Fig. 9). However, a small temporal offset (< 150 years) was observed for different zonations of CPT and CC profiles (Fig. 9). The temporal variations in magnetic proxy of CPT and CC profiles were very small and broadly fall within the measurement accuracy of the AMS ^{14}C chronology and cannot be resolved. No significant spatial variation in concentration of magnetic minerals was found in the CPT and CC profiles except for two intervals i.e. ~ 1150 to 770 cal years BP and ~ 390 cal years BP to present (Fig. 9). The relatively high concentration of magnetic minerals in the CC during these periods was possibly due to higher sedimentation rates and sediment focusing mechanism.

However, TOC showed a contrasting pattern in CC and CPT profiles for the period between ~ 770 cal years BP and Present. The spatial variations in the organic proxies such as TOC had been well reported by several workers (Johnson et al. 2012; Wang et al. 2009). A higher TOC percentage was observed for the marginal trench as compared to the depocenter core for the same period. Generally, higher TOC along with higher sedimentation had been reported in the depocenter part of the lake due to sediment focusing mechanisms (Davis and Ford 1982; Hilton 1985; Wang et al. 2009). The contrasting behavior in the present lake

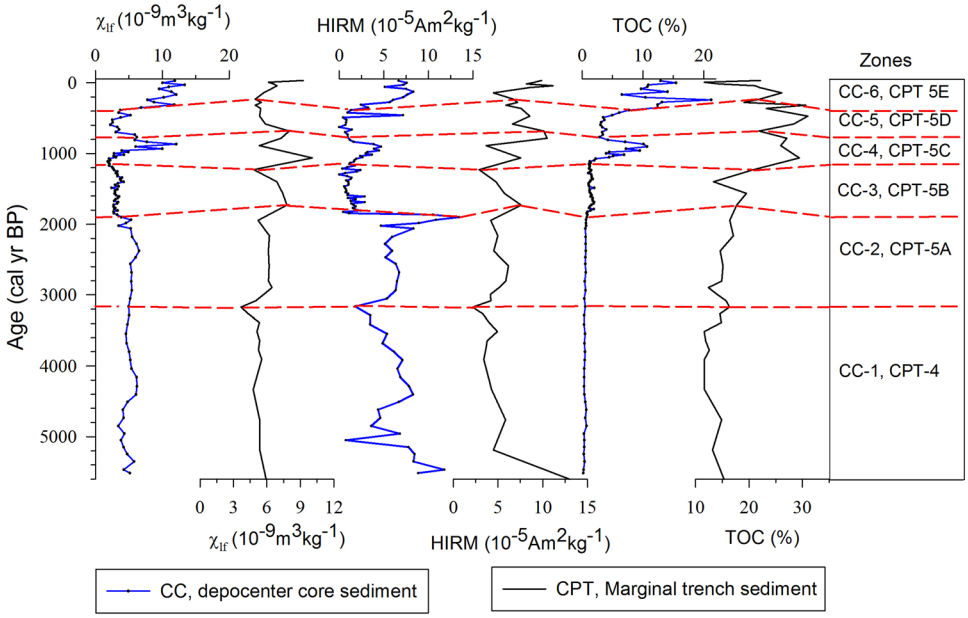

Fig. 9 Comparison of environmental magnetic parameters and total organic carbon of the depocenter CC and shore CPT profiles. The CPT data are after Rawat et al. (2015a, b)

is possibly due to the development of peat on the lake margins that has led to higher organic carbon in the marginal trench. Further, major and minor inter-core variability has been often assigned to varying accuracy of the chronological model and varying sampling resolutions between different cores (Fritz et al. 2006; Bogotá-A et al. 2011). Such complexities were precluded as sampling resolutions were kept the same for the core and marginal trench (i.e. 1 cm interval) and similar accuracies were achieved for the AMS ^{14}C analysis. Therefore, observed spatial variation is likely due to the development of peat in the margins. Further, the depocenter has high sedimentation thus representing high-resolution data as well as TOC and magnetic data co-varies in the depocenter. This implies that TOC data in recent sediments are more suitable for paleoclimate reconstruction from the depocenter cores in cases of the development of peats on lake margins. The present study suggested that despite the spatial differences in the sedimentation rate, the magnetic properties of core and trench samples indicated similar variations over equivalent time periods. The depocenter and shore margin site data comparison in a small lake indicated that depocenter core provides high-resolution lacustrine environment, whereas the shore margin trench records major shifts in paleoclimate over a longer time scale and is consistent with the similar observations in case of large size lakes (Wang et al. 2009). Therefore, based on present study we recommend that depocenter of lake should be selected as a site of interest for sample collection to obtain high-resolution paleoclimate data whereas shore margin site should be selected as a site of interest to obtain long-term paleoclimate at coarser resolution.

Magnetic mineral sources in lake sediments

The magnetic mineral sources into this lake have been suggested to be from the lake catchment and no significant post-depositional alteration such as dissolution of magnetic minerals and/or from authigenic and biogenic processes were reported from the marginal CPT profile (Rawat et al. 2015b). The new data on hysteresis analysis of several samples at various depth showed dominant ferrimagnetic behavior of lake sediments which was affirmed by the IRM un-mixing data indicating low coercivity pedogenic magnetite and medium coercivity partially oxidized magnetite/maghemite as dominant magnetic carriers. Lake sediments were also composed of high coercivity antiferromagnetic mineral, such as, hematite but in relatively low proportions. Temperature-dependent magnetic susceptibility results did not show the presence of greigite indicating no alteration of magnetic signals from authigenic greigite formation. The IRM un-mixing data also did not show any sign of bacterial magnetite often characterized with low DP values < 0.19. However, IRM un-mixing is not a distinctive method to characterize bacterial magnetite and requires more detailed investigation using transmission electron microscopy (TEM), which is out of scope/aim of the present study. Therefore, we assume that most magnetic signals in lake sediments are from the catchment soils. The dissolution behavior in lake sediments is often described from decreasing concentration of fine magnetic particles with depth. In the present studied lake sediments, low χ_{ARM} was found from ~ 1200 to 5510 cal years BP. However, during this period sediments were also characterized by low TOC, an important catalyst for reducing environment and dissolution. Further, Mn/Fe ratio was

relatively high from ~ 2200 to 5510 cal years BP indicating more oxidizing condition during this period. Therefore, sediments during this period did not show a signal of dissolution but were rather dominated by high coercivity minerals than low coercivity minerals as shown by low S-ratio values. The ISM and westerlies are sources of moisture for this lake. A recent study from the region had shown that fine sediment particles could be brought by westerly winds as dust deposition (Kumar et al. 2020). Therefore, fine-grained hematite could also be sourced from dust. However, during the period (~ 5500 to 2000 cal years BP) of relative abundance of antiferromagnetic minerals, the strength of westerlies had weakened and ISM was dominant (Kumar et al. 2020). Therefore, it appears that all magnetic minerals were from catchment soils and their concentration could be used to infer the strength of ISM.

Mid- to late Holocene climatic variability in the Lahaul, NW Himalaya

The decreased HIRM, low TOC and decreased Al/Na, Al/Mg and CIA during ~ 5500 to 3160 cal years BP indicated an overall low influx of sediments, low organic productivity and low chemical weathering in the catchment suggesting relatively weak strength of the ISM (Fig. 10). The period from ~ 5500 to 3160 cal years BP can be subdivided into middle Holocene (~ 5500 to 4200 cal years BP) and late Holocene/Meghalayan stage (~ 4200 cal years BP to Present). Various paleoclimatic records from the Indian subcontinent showed that period from ~ 5500 to 4200 cal years BP (and in some studies up to 3900 cal years BP) was characterized by increased ISM precipitation and/or as a relatively stable warm and wet climatic period (e.g. Kathayat et al. 2017; Dixit et al. 2018; Rawat et al. 2021a). This warm and wet period is explained as late portion of mid Holocene climate optimum (mHCO). The abrupt decline in strength of ISM at ~ 4200 cal years BP has been reported in many studies (e.g. Staubwasser et al. 2003; Dixit et al. 2014; 2018; Dutt et al. 2018; Singh et al. 2021). The time period from ~ 5200 to 3300 cal years BP is important in context of understanding past civilizations and climate relationship. The early agricultural based establishment of the Indus valley civilization (IVC) between ~ 5200 and 4500 cal years BP has been suggested to be favored by stable warm-wet climatic condition whereas decline in ISM precipitation during mature/late phase of the IVC led to the de-urbanization of the IVC between ~ 3900 and 3300 cal years BP (Dixit et al. 2018; Dutt et al. 2018; Pokharia et al. 2017, 2020; Rawat et al. 2021a). However, the nature and timing of this late Holocene decline in ISM precipitation is not uniform across various basins in the Indian subcontinent with many records showing decline in ISM precipitation between ~ 4600 and 3900 cal years BP (e.g. Dutt et al. 2019; Dixit et al. 2018;

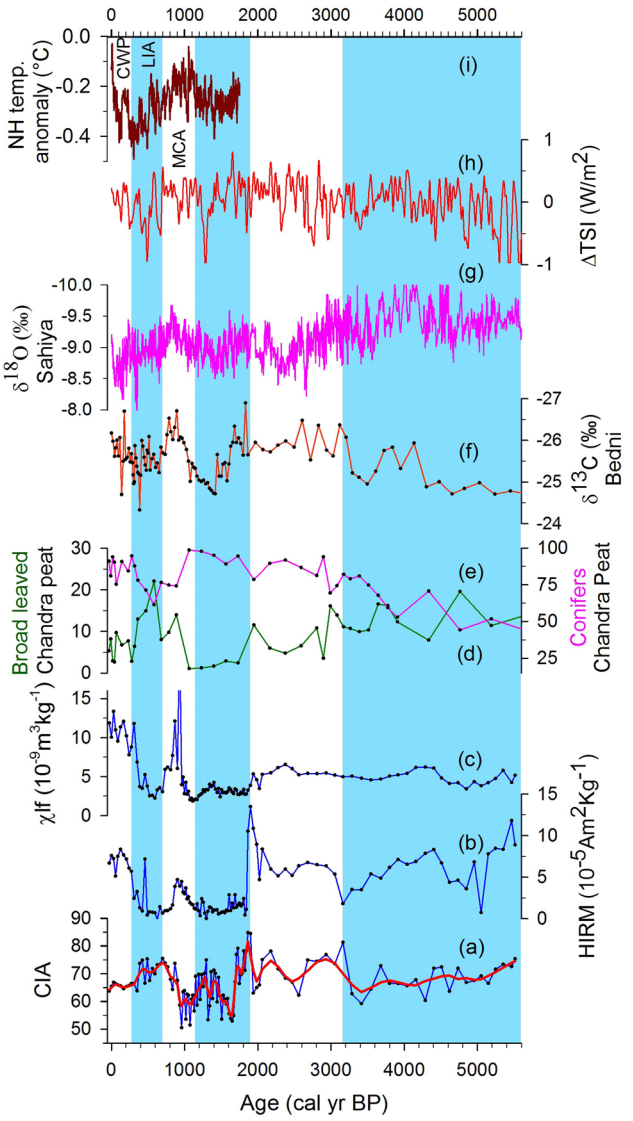

Fig. 10 Comparison of multi-proxy (CIA, HIRM and χ_{lf}) (**a–c**) results of the depocenter CC with **d**–e Broadleaved and Conifer pollen data from marginal shore CPT sites of the Chandra lake, Lahaul (Rawat et al. 2015a), **f** carbon isotope data from Bednikund lake, Garhwal Himalaya (Rawat et al. 2021a and b), **g** oxygen isotope data from Shaiya cave speleothem, Garhwal Himalaya (Kathayat et al. 2017), **h** total solar irradiance (Steinhilber et al. 2009) and **i** NH temperature anomaly (Mann and Jones 2003)

Kotlia et al. 2015; Rawat et al. 2021a) and with several studies showing non-abrupt nature of this decline in ISM precipitation (e.g. Kathayat et al. 2017). New evidence from Arabian Sea core suggested that both Indian winter monsoon (IWM) (from westerly) and ISM had declined at ~ 4100 cal years BP (Giesche et al. 2019). Several studies also contest records of stable warm and wet climate between ~ 5500 and 4200 cal years BP with weakened/decreased ISM precipitation during this period (e.g. Srivastava et al. 2017a, b; Prasad et al. 2014, 2020; Ali et al. 2020;

Wang et al. 2020). The pollen record from the marginal trench profile of the studied lake showed the effective growth of meadow vegetation between ~ 6700 and 3300 cal years BP under relatively warm-wet climate condition and was interrupted by an intermittent cold and dry climatic period between ~ 4800 and 4300 cal years BP (Rawat et al. 2015a). To have more local perspective on ISM variations during this period climatic records from NW and Central Himalaya is discussed. The multi-proxy record from neighboring lake in the Chandra valley showed intensified ISM strength from ~ 6500 to 4500 cal years BP, whereas from ~ 4500 to 3900 cal years BP precipitation source shifted to westerlies which further dominated up to 3000 cal years BP with region experiencing more colder and drier climatic condition (Kumar et al. 2020). Shamurailatpam et al. (2020) based on organic productivity record also showed decreased ISM precipitation in the Chandra valley between ~ 5800 and 3800 cal years BP. In the same basin of Lahaul Himalaya, environmental magnetic records from Triloknath paleolake sediments showed decreased magnetic mineral concentration between ~ 5400 and 3900 cal years BP suggesting reduced monsoon season with less warm climatic conditions (Bali et al. 2017). The multi-proxy records from Kilang Sarai, Lahaul Himalaya also suggested the prevalence of cold and dry climatic conditions between ~ 4500 and 2000 cal years BP (Bohra and Kotlia 2015). The regional records from further NW of the present studied site also indicated a cold-dry climate and weak ISM strength during this period. For example, extensively studied lake core records from the Tso Moriri, Ladakh had shown a progressive lowering of lake water level, reduction in detrital input, increase in the authigenic calcite precipitation as well as increase in salinity during ~ 5500 to 2700 cal years BP, which indicated higher summer evaporation than fresh water input (low ISM precipitation + melt water) (Mishra et al. 2015a, b and 2018). Pollen records from Tso Moriri lake also suggested that dry climatic conditions prevailed in the region at around ~ 4000 cal years BP which continued up till ~ 3600 cal years BP (Leipe et al. 2014). Sedimentological and geochemical record from sediments of the Tso Moriri lake showed long cold and arid phase between ~4350 and 3450 cal years BP (Dutt et al. 2018). The glacial advances in the Tso Moriri region have also been noted during this period (Hedrick et al. 2011; Leipe et al. 2014). The pollen record from the Tso Kar lake in Trans Himalaya, which falls in similar climatic conditions as of Tso Moriri, showed humid climate from ~ 6900 to 4800 cal years BP followed by expansion of Chenopodiaceae dominated desert-steppe after ~ 4800 cal years BP indicating dry climatic condition (Demske et al. 2009). The multi-proxy data also showed shallowing of Tso kar lake after ~ 5500 cal years BP with pronounced aridity from ~ 4800 to 4200 cal years BP (Wünnemann et al. 2010). The weakening phases of summer monsoon in the Ladakh, Himalaya also corresponded to increased strengths of the westerlies (Demske et al. 2009). The glacier advance in the semi-arid Gomuche Kangri, Karzok valley, Zanskar from ~ 6100 to 3300 cal years BP also indicated the prevalence of cold-dry conditions (Saha et al. 2018). This cold-dry period is associated with the North-Atlantic cooling and likely tele-connected via mid-latitude westerlies (Saha et al. 2018). However, contrastingly Kumar et al. (2020) suggested that moisture source for glaciation in NW Himalaya during ~ 6500 to 4500 cal years BP was from the ISM. Phartiyal et al. (2020) found cold and dry climate between ~ 5800 and 4400 cal years BP in Khardung La region of the Ladakh-Karakoram. Whereas in another study from the same region Phartiyal et al. (2021) reported a wet climate and westerly dominated precipitation from ~ 4100 to 3000 cal years BP. Ali et al. (2020) showed a cold-dry climatic condition with reduced ISM precipitation from ~ 6200 to 4500 cal years BP and a warm-wet climate with increased ISM precipitation from ~ 4500 to 3400 cal years BP in the Zanskar valley of NW Himalaya. Shah et al. (2020) found a wet climatic condition from ~ 6350 to 5000 cal years BP and a dry climatic condition from ~ 5000 to 4000 cal years BP in the Kashmir valley and assigned these climatic changes to increasing and decreasing strengths of westerlies precipitation, respectively. Lone et al. (2020) also found warm-wet climatic condition in the Kashmir valley from ~ 6000 to 3900 cal years BP and a cold-dry climate from ~ 3900 to 2500 cal years BP and suggested these climatic variability to changing strengths of westerly precipitation. Quamar (2019) showed increased ISM precipitation strength between ~ 5300 and 2800 cal years BP in the Jammu region of the NW Himalaya. In the central-western Himalayan region, the weakening of the ISM has been recorded between ~ 4000 and 3500 cal years BP (Phadtare 2000). The multi-proxy study on a peat sequence from the Alaknanda basin also recorded declined ISM precipitation between ~ 5400 and 3800 cal years BP (Srivastava et al. 2017a). Weak ISM strength from ~ 5800 to 5000 and strengthen ISM from ~ 5000 to 4000 cal years BP was reported from Benital lake in Pinder valley (Bhushan et al. 2018). Recent high-resolution study from Bednikund in Pinder valley showed stable warm and wetclimate from ~ 6000 to 3950 anddecreasedISM precipitation from ~ 3950 to3380 cal years BP (Rawat et al. 2021a). A number of paleoclimatic studies have been carried out from NW and central Himalaya and from above synthesis it indicates that variability in climate has not been uniform in different basins between ~ 5500 and 3000 cal years BP and sources of precipitation i.e. ISM and westerlies have not been well quantified. The isotopic composition of modern Indus river head water in Ladakh showed dominant ISM contribution (~ 74%) and minor Mediterranean source/westerlies contribution (~ 26%) in the Indus River (Sharma et al. 2017). Whereas

moisture source determination from pore water, lake surface water and glacier using deuterium excess showed dominant Mediterranean source in Lahaul Himalaya during Holocene (Kumar et al. 2020). The climatic variability in NW Himalaya is complicated as it receives moisture from both ISM and westerlies and therefore only strength determination of precipitation is not important but also identification of different sources of moisture in different basins is important for more accurate understanding of the ISM dynamics in the NW Himalaya during middle Holocene.

The increased influx of antiferromagnetic minerals was recorded by an increase in HIRM during ~ 3160 to 1900 cal years BP. The increased values of Al/Na, Al/Ca, Al/Mg, Al/Ti, Ti/Na and CIA showed higher chemical weathering of catchment rocks (Fig. 10). The pollen results from the marginal CPT site showed the mixed coniferous and broad leaved forest along with the growth of diverse vegetation cover in the region and continuous improvement in wetland taxa between ~ 3260 and 1950 cal years BP under warm and wet climatic conditions (Rawat et al. 2015a) (Fig. 10d, e). In the NW Himalayan region of Ladakh, several studies showed a cold and dry climate between ~ 3200 and 2000 cal years BP (e.g. Demske et al. 2009; Wünnemann et al. 2010; Leipe et al. 2014; Lone et al. 2020), whereas few studies record relatively warm and wet climate during this period (Ali et al. 2020; Phartiyal et al. 2020; Quamar 2019). Further, in northwestern-central Himalayan region most studies showed warm and wet climate in different basins during ~ 3200 to 2000 cal years BP (Phadtare 2000; Kotlia and Joshi 2013; Bhushan et al. 2018; Shamurailatpam et al. 2020; Rawat et al. 2021a) (Fig. 10). Based on various studies in NW-central Himalaya, a general census can be reached for the overall warm and wet climatic condition between ~ 3200 and 2000 cal years BP.

The decreased influx of magnetic minerals shown by decreased χ_{lf}, SIRM and HIRM values in the Chandra core from ~ 1900 to 1150 cal years BP indicated decreased supply of magnetic minerals in response to the decreased ISM precipitation (Fig. 10). The decreased CIA, Al/Na and Ti/Na showed lower chemical weathering of catchments. High Rb/Sr was found during this period corresponding with maximum sedimentation implying higher physical weathering. TOC data showed lower lake and catchment productivity prompting more erosion and lake-fill up. The relative decline of broad leaved and meadow taxa and the prolific increase of coniferous taxa in the region during ~ 1950 to 1060 cal years BP suggested a cool and moist climate (Rawat et al. 2015a) (Fig. 10d, e). The pollen record from the neighboring Spiti valley also indicated cool-dry climatic conditions between ~ 2000 and 1000 cal years BP (Mazari et al. 1995). Kar et al. (2002) found cool-moist climate between ~ 2500 and 1700 cal years BP in the central-western Garhwal Himalaya. In the Dhakuri region of Pinder basin, drier climatic condition was reported at ~ 1600 cal years BP (Rühland et al. 2006). The cold-dry climate in the Chamoli region of the Pinder basin had prevailed from ~ 1860 to 1050 cal years BP (Rawat et al. 2021a) (Fig. 10f). The pollen analysis of Dewar Tal sediments also showed climatic deterioration between ~ 2000 and 1400 cal years BP (Chauhan and Sharma 2000). The lake sediments from Badani Tal showed low organic productivity, less erosion and reduced rainfall under semi-arid to arid climate *ca.* 1800 to 920 cal years BP (Kotlia and Joshi 2013). Recently, Srivastava et al. (2020) also recorded extreme aridity between ~ 2000 and 1000 cal years BP which led to ~ 6 m lake level fall in Pangong Tso in the Ladakh, NW Himalaya. Emerging evidences indicate a decline in ISM precipitation between ~ 2000 and 1000 cal years BP in the NW and central Himalaya. The Northern Hemisphere (NH) temperature data recorded cooler climate during this period which is in accordance with reduced ISM strength (Fig. 10i) (Mann and Jones 2003).

The abundance of organic matter shown by increased TOC in the Chandra core from ~ 1150 to 770 cal years BP (~ 800 to 1180 AD) coincided with the increased magnetic mineral concentrations represented by increased values of χ_{lf}, χ_{fd}, SIRM, χ_{ARM} and HIRM (Fig. 10). The increased SP ferrimagnetic particle concentration during this period indicated higher pedogenesis under favorable warm and wet climatic conditions. The increased Li/Ba ratio during this period indicated higher chemical weathering and increased Mn/Fe showed relatively oxidizing condition. Al/Na, Al/Ca, Al/Mg, Al/Ti, Ti/Na and CIA showed low/decreased values during this period implying lower chemical weathering of catchment rocks under reduced precipitation, which is in contrast with the magnetic, TOC and Li/Ba data suggesting relatively warm and wet climate. TOC data of marginal trench and depocenter core showed maximum vegetation growth in lake and catchment during this period. The higher vegetation growth in lake margins may have restricted the outflow of the lake leading to higher retention of liable (i.e. Na, Ca and K) elements compared to Al. This implies that lake may have started showing closed lake basin behavior. Therefore, as discussed above, reverse CIA and Al/element ratios can be applied from this period forward with their lower values showing higher chemical weathering of catchment rocks. The pollen record from the CPT section also showed expansion of broad leaved, non-arboreal pollens and fern taxa between ~ 1160 and 650 cal years BP, which indicated warm and wet climatic condition in the Lahaul valley (Rawat et al. 2015a) (Fig. 10d, e). Overall this period was marked by high lake productivity, enhanced pedogenesis, higher chemical weathering and increased runoff that indicated strengthened ISM. This warm and wet phase of ~ 380 years (~ 1150 to

770 cal years BP) corresponded to the "Medieval Climate Anomaly" (MCA). The total solar irradiance (TSI) and NH temperature showed covariance with the proxy data indicating warmer period corresponded with higher ISM precipitation (Fig. 10h, i). The warm and wet MCA has been recorded in numerous NW Himalayan basins e.g. between ~ 1500 and 900 cal years BP in the Lahaul and Spiti valley (Chauhan et al. 2000) and between ~ 1300 and 800 cal years BP in the Parvati valley (Chauhan 2006). In the central-western Himalaya, the MCA has been recorded between ~ 1200 and 700 cal years BP in the Alaknanda basin, Garhwal Himalaya (Srivastava et al. 2017a), and between ~ 1200 and 800 cal years BP in Sahiya cave, Garhwal Himalaya (Kathayat et al. 2017) (Fig. 10g). In the Pinder basin, MCA was recorded between ~ 1050 and 760 years BP (Rawat et al. 2021a) (Fig. 10f). The higher flood frequencies in Himalayan Rivers have also been recorded during the MCA (Srivastava et al. 2017b).

The decreased values of magnetic concentration parameters (χ_{lf}, χ_{fd}, SIRM, χ_{ARM} and HIRM) between ~ 770 and 390 cal years BP (~ 1180–1560 AD) showed low supply of magnetic minerals under declined precipitation condition (Fig. 10). Further, decreased TOC during this period also indicated low paleo-productivity implying climatic deterioration. The decreased Li/Ba indicated lower chemical weathering. The high CIA, Al/Na, Al/Ca, Al/Mg, Al/Ti and Ti/Na under reverse behavior indicated lower chemical weathering due to reduced precipitation condition. The pollen records from marginal CPT site showed a decline in broad leaved and meadow vegetation during ~ 650 to 340 cal years BP (~ 1300–1610 AD) (Rawat et al. 2015a) (Fig. 10d, e). The overall climate during this period in the Chandra valley, Lahaul Himalaya was cold and dry with reduced ISM precipitation. This cold-dry period corresponded to the most recent climatic event, the "Little Ice Age" (LIA). The TSI and NH temperature data correlates well with the proxy data during this period (Fig. 10h, i). The LIA has been reported from several parts of the NW Himalaya (Bhattacharyya 1988; Mazari et al. 1995; Chauhan et al. 2000; Chauhan 2006) and the central-western Himalaya (Bhattacharyya and Chauhan 1997; Kar et al. 2002; Kathayat et al. 2017; Shekhar et al. 2017; Saha et al. 2018; Rawat et al. 2021a). During this period, glaciers in the NW Himalaya have advanced (Owen et al. 1996; Rowan 2017; Saha et al. 2018).

The subsequent period after ~ 390 cal years BP to the present was marked by increasing trend in magnetic mineral concentration (increased χ_{lf}, χ_{fd}, SIRM, χ_{ARM} and HIRM), TOC, Li/Ba and declining trend in Al/Na, Al/Ca, Al/Mg, Al/Ti, Ti/Na and CIA suggesting increased magnetic mineral supply, increased lake and catchment productivity and higher chemical weathering under climatic amelioration and set towards modern current warm period (CWP).

Conclusions

The present study was aimed to understand the inter-site spatial and temporal variations in the inorganic and organic proxies in a small post-glacial lake from the Lahaul Himalaya and to reconstruct paleoenvironmental variations during the middle to late Holocene. The inter-site comparison between depocenter core and marginal shore trench indicated distinct sedimentation rate with ~ 2.5 times higher in the former. Despite the spatial differences in the sedimentation rate, the magnetic properties of core and trench samples indicated similar environmental signals over equivalent time periods. The higher percentage of total organic carbon was found in the marginal trench as compared to the depocenter core defying sediment focusing mechanism possibly due to the development of peat at lake margins. The environmental magnetic, geochemical and total organic carbon data of the depocenter core provided significant information on erosion, chemical weathering and productivity of the lake catchment of the Chandra valley during middle to late Holocene in response to changing strength of the ISM. The weak ISM strengths in the Lahaul Himalaya had been recorded during periods (1) ~ 5500 to 3160 cal years BP, (2) ~ 1900 to 1150 cal years BP, and (3) ~ 770 to 390 cal years BP. The strengthening or relatively improved ISM conditions were recorded during intermediate intervals (1) ~ 3160 to 1900 cal years BP, (2) ~ 1150 to 770 cal years BP, and (3) ~ 390 cal years BP to the Present (1950 AD). The weakened and strengthened ISM periods during middle to late Holocene in the Lahaul Himalaya were in accordance with the regional climatic variability of various other NW and central Himalayan basins.

Supplementary Information The online version contains supplementary material available at https://doi.org/10.1007/s10201-021-00669-9.

Acknowledgements We thank Director, Wadia Institute of Himalayan Geology and Head, Department of Geology, University of Pune for providing necessary working facilities. We acknowledge Dr. NR Phadtare for his help during the field work and Dr. PP Khanna and Dr. Shailesh Aggarwal for their help in geochemical measurements. We are thankful to Dr. Yogesh Kulkarni (GIT, India) and Mr. Saurabh Singh (JNU, India) for map preparation and discussion. We thank two anonymous reviewers for their insightful comments which helped in improving the overall quality and clarity of the paper. We also thank Editors Prof. Ichiro Tayasu and Jorge García Molinos for careful handling of the manuscript.

Author contributions Conceptualization: SR, AKG and PS; sampling: SR and SJS; data curation: SR and PS; formal analysis: SR and PS; interpretation: PS, SR, AKG, LJ and SJS; writing—original draft: PS, SR, AKG and SJS; writing—review and editing: PS, SR and LJ.

Funding SR and SJS acknowledge Department of Science and Technology (DST), India project grant (SR/S4/ES-130/2004). SR acknowledges DST, India project grant ECR/2017/001046. AKG acknowledges J.C. Bose fellowship (SR/S2/JCB-80/2011). SJS acknowledges

DST-FIST grant SR/FST/ESII-101/2010. PS is supported by Fundação de Amparo a Pesquisa do Estado de São Paulo (FAPESP) project 2019/11364-0 and LJ by FAPESP project 2016/24946-9.

Data availability All the data reported in the research article are provided in the manuscript and supplementary files.

References

Ali SN, Agrawal S, Sharma A, Phartiyal B, Morthekai P, Govil P, Bhushan R, Farooqui S, Jena PS, Shivam A (2020) Holocene hydroclimatic variability in the zanskar valley, northwestern Himalaya, India. Quat Res 97:140–156

Anderson NJ (1990) Variability of diatom concentrations and accumulation rates in sediments of a small lake basin. Limnol Oceanogr 35:497–508

Bali R, Khan I, Sangode SJ, Mishra AK, Ali SN, Singh SK, Tripathi JK, Singh DS, Srivastava P (2017) Mid-to late Holocene climate response from the Triloknath palaeolake, Lahaul Himalaya based on multiproxy data. Geomorphology 284:206–219

Bhargava ON, Srivastava RN, Gadhoke SK (1991) The proterozoic-palaeozoic spiti sedimentary basin. Sedimentary Basins of India. In: Tectonic context. Gyanodaya Prakashan, Nainital, p 236–260

Bhattacharyya A (1988) Vegetation and climate during postglacial period in the vicinity of Rohtang Pass, Great Himalayan Range. Pollen Spores 30:417–427

Bhattacharyya A, Chauhan MS (1997) Vegetational and climatic changes during recent past around Tipra bank glacier, Garhwal Himalaya. Curr Sci 72:408–412

Bhushan R, Sati SP, Rana N, Shukla AD, Mazumdar AS, Juyal N (2018) High-resolution millennial and centennial scale Holocene monsoon variability in the Higher Central Himalayas. Palaeogeogr Palaeoclimatol Palaeoecol 489:95–104

Blaauw M, Christen JA (2011) Flexible paleoclimate age-depth models using an autoregressive gamma process. Bayesian Anal 6:457–474

Bogotá-A RG, Groot MHM, Hooghiemstra H, Lourens LJ, Van der Linden M, Berrio JC (2011) Rapid climate change from north Andean Lake Fúquene pollen records driven by obliquity: implications for a basin-wide biostratigraphic zonation for the last 284 ka. Quat Sci Rev 30:3321–3337

Bohra A, Kotlia BS (2015) Tectono-climatic signatures during Late Quaternary in the Yunam basin, Baralacha Pass (upper Lahaul valley, India), derived from multi-proxy records. Quat Int 371:111–121

Burbank DW (1982) Rapid late Pleistocene uplift rates from the Pir Panjal range, northwestern Himalaya. In: Seventh AMQUA conference proceeding, Abstract, p 78

Charles DF, Dixit SS, Cumming BF, Smol JP (1991) Variability in diatom and chrysophyte assemblages and inferred pH: paleolimnological studies of Big Moose Lake, New York, USA. J Paleolimnol 5:267–284

Chauhan MS (2006) Late Holocene vegetation and climate change in the alpine belt of Himachal Pradesh. Curr Sci 91:1562–1567

Chauhan MS, Sharma C (2000) Late Holocene vegetation and climate in Dewar Tal area, Inner Lesser Garhwal Himalaya. Palaeobotanist 49:509–551

Chauhan MS, Mazari RK, Rajagopalan G (2000) Vegetation and climate in upper Spiti region, Himachal Pradesh during late Holocene. Curr Sci 79:373–377

Chen J, An Z, Head J (1999) Variation of Rb/Sr ratios in the loess-paleosol sequences of central China during the last 130,000 years and their implications for monsoon paleoclimatology. Quat Res 51:215–219

Condie KC, Dengate J, Cullers RL (1995) Behavior of rare earth elements in a paleoweathering profile on granodiorite in the Front Range, Colorado, USA. Geochim Cosmochim Acta 59:279–294

Davis MB, Ford MS (1982) Sediment focusing in Mirror Lake, New Hampshire. Limnol Oceanogr 27:137–150

Dekkers MJ (1990) Magnetic properties of natural goethite—III. Magnetic behaviour and properties of minerals originating from goethite dehydration during thermal demagnetization. Geophys J Int 103:233–250

Demske D, Tarasov PE, Wünnemann B, Riedel F (2009) Late glacial and Holocene vegetation, Indian monsoon and westerly circulation in the Trans-Himalaya recorded in the lacustrine pollen sequence from Tso Kar, Ladakh, NW India. Palaeogeogr Palaeoclimatol Palaeoecol 279:172–185

Dixit Y, Hodell DA, Petrie CA (2014) Abrupt weakening of the summer monsoon in northwest India~ 4100 yr ago. Geology 42:339–342

Dixit Y, Hodell DA, Giesche A, Tandon SK, Gazquez F, Saini HS, Skinner LC, Mujtaba SA, Pawar V, Singh RN, Petrie CA (2018) Intensified summer monsoon and the urbanization of Indus Civilization in northwest India. Sci Rep 8:4225. https://doi.org/10.1038/s41598-018-22504-5

Dunlop DJ (2002) Theory and application of the Day plot (Mrs/Ms versus Hcr/Hc) 1. Theoretical curves and tests using titanomagnetite data. J Geophys Res Solid Earth. https://doi.org/10.1029/2001JB000487

Dutt S, Gupta AK, Wünnemann B, Yan D (2018) A long arid interlude in the Indian summer monsoon during~ 4,350 to 3,450 cal. yr BP contemporaneous to displacement of the Indus valley civilization. Quatern Int 482:83–92

Dutt S, Gupta AK, Singh M, Jaglan S, Saravanan P, Balachandiran P, Singh A (2019) Climate variability and evolution of the Indus civilization. Quat Int 507:15–23

Fedo CM, Wayne Nesbitt H, Young GM (1995) Unraveling the effects of potassium metasomatism in sedimentary rocks and paleosols, with implications for paleoweathering conditions and provenance. Geology 23:921–924

Fedotov AP, Phedorin MA, De Batist M, Ziborova GA, Kazansky AY, Semenov MY, Matasova GG, Khabuev AV, Kugakolov SA, Rodyakin SV, Krapivina SM (2008) A 450-ka long record of glaciation in Northern Mongolia based on studies at Lake Khubsugul: high-resolution reflection seismic data and grain-size variations in cored sediments. J Paleolimnol 39:335–348

Finsinger W, Belis C, Blockley SP, Eicher U, Leuenberger M, Lotter AF, Ammann B (2008) Temporal patterns in lacustrine stable isotopes as evidence for climate change during the late glacial in the Southern European Alps. J Paleolimnol 40:885–895

Fritz CS, Baker PA, Tapia P, Garland J (2006) Spatial and temporal variation in cores from Lake Titicaca, Bolivia/Peru during the last 13,000 yrs. Quat Int 158:23–29

Gälman V, Rydbergde-Luna JSS, Bindler Renberg RI (2008) Carbon and nitrogen loss rates during aging of lake sediment: changes over 27 years studied in varved lake sediment. Limnol Oceanogr 53:1076–1082

Gälman V, Rydberg J, Bigler C (2009) Decadal diagenetic effects on δ13C and δ15N studied in varved lake sediment. Limnol Oceanogr 54:917–924

Garnier JM, Garnier J, Debnath P, Prado LF, Yokoyama E, Das RK, Mathé PE, Islam MS (2020) Late Holocene paleoenvironmental records in Eastern Bangladesh from lake sediments: a multiproxy approach. Quat Int 558:39–46

Gasse F, Fontes JC, Van Campo E, Wei K (1996) Holocene environmental changes in Bangong Co Basin (Western Tibet), Part 4:

discussion and conclusion. Palaeogeogr Palaeoclimatol Palaeoecol 120:79–82
Giesche A, Staubwasser M, Petrie CA, Hodell DA (2019) Indian winter and summer monsoon strength over the 4.2 ka BP event in foraminifer isotope records from the Indus River delta in the Arabian Sea. Clim past 15:73–90
Hanesch M, Stanjek H, Petersen N (2006) Thermomagnetic measurements of soil iron minerals: the role of organic carbon. Geophys J Int 165:53–61
Hedrick KA, Seong YB, Owen LA, Caffee MW, Dietsch C (2011) Towards defining the transition in style and timing of Quaternary glaciation between the monsoon-influenced Greater Himalaya and the semi-arid Trans Himalaya of Northern India. Quat Int 236:21–33
Hilton J (1985) A conceptual framework for predicting the occurrence of sediment focusing and sediment redistribution in small lakes. Limnol Ocenaogr 30:1131–1143
Hilton J, Lishman JP, Allen PV (1986) The dominant processes of sediment distribution and focusing in a small, eutrophic, monomictic lake. Limnol Oceanogr 31:125–133
Hodell DA, Brenner M, Kanfoush SL, Curtis JH, Stoner JS, Xueliang S, Yuan W, Whitmore TJ (1999) Paleoclimate of southwestern China for the past 50,000 yr inferred from lake sediment records. Quat Res 52:369–380
Jin Z, Wang S, Shen JI, Zhang E, Li F, Ji J, Lu X (2001) Chemical weathering since the Little Ice Age recorded in lake sediments: a high-resolution proxy of past climate. Earth Surf Proc Landf 26:775–782
Jin Z, Cao J, Wu J, Wang S (2006) A Rb/Sr record of catchment weathering response to Holocene climate change in Inner Mongolia. Earth Surf Proc Landf 31:285–291
Johnson TC, Van Alstine JD, Rolfhus KR, Colman SM, Wattrus NJ (2012) A high resolution study of spatial and temporal variability of natural and anthropogenic compounds in offshore Lake Superior sediments. J Great Lakes Res 38:673–685
Jordanova D, Jordanova N (2016) Thermomagnetic behavior of magnetic susceptibility-heating rate and sample size effects. Front Earth Sci 3:90. https://doi.org/10.3389/feart.2015.00090
Jovane L, Florindo F, Acton G, Ohneiser C, Sagnotti L, Strada E, Verosub KL, Wilson GS, Iacoviello F, Levy RH, Passchier S (2019) Miocene glacial dynamics recorded by variations in magnetic properties in the ANDRILL-2A drill core. J Geophys Res Solid Earth 124:2297–2312
Kar A, Ranhotra PS, Bhattacharyya A, Sekar B (2002) Vegetation vis-a-vis climate and glacial fluctuations of the Gangotri glacier since the last 2000 years. Curr Sci 82:347–351
Kathayat G, Cheng H, Sinha A, Yi L, Li X, Zhang H, Li H, Ning Y, Edwards RL (2017) The Indian monsoon variability and civilization changes in the Indian subcontinent. Sci Adv. https://doi.org/10.1126/sciadv.1701296
Kirby ME, Poulsen CJ, Lund SP, Patterson WP, Reidy L, Hammond DE (2004) Late Holocene lake level dynamics inferred from magnetic susceptibility and stable oxygen isotope data: Lake Elsinore, southern California (USA). J Paleolimnol 31:275–293
Kotlia B, Joshi L (2013) Late Holocene climatic changes in Garhwal Himalaya. Curr Sci 104:911–919
Kotlia BS, Singh AK, Joshi LM, Dhaila BS (2015) Precipitation variability in the Indian Central Himalaya during last ca. 4,000 years inferred from a speleothem record: Impact of Indian Summer Monsoon (ISM) and Westerlies. Quat Int 371:244–253
Kumar O, Ramanathan AL, Bakke J, Kotlia BS, Shrivastava JP (2020) Disentangling source of moisture driving glacier dynamics and identification of 82 ka event: evidence from pore water isotopes, Western Himalaya. Sci Rep 10:15324. https://doi.org/10.1038/s41598-020-71686-4
Leipe C, Demske D, Tarasov PE (2014) A Holocene pollen record from the northwestern Himalayan lake Tso Moriri: Implications for palaeoclimatic and archaeological research. Quat Int 348:93–112
Liu J, Chen J, Selvaraj K, Xu Q, Wang Z, Chen F (2014) Chemical weathering over the last 1200 years recorded in the sediments of Gonghai Lake, Lvliang Mountains, North China: a high-resolution proxy of past climate. Boreas 43:914–923
Lone AM, Achyuthan H, Shah RA, Sangode SJ, Kumar P, Chopra S, Sharma R (2020) Paleoenvironmental shifts spanning the last~ 6000 years and recent anthropogenic controls inferred from a high-altitude temperate lake: Anchar Lake, NW Himalaya. Holocene 30:23–36
Lu Y, Meyers PA, Eadie BJ, Robbins JA (2010) Carbon cycling in Lake Erie during cultural eutrophication over the last century inferred from the stable carbon isotope composition of sediments. J Paleolimnol 43:261–272
Mann ME, Jones PD (2003) Global surface temperatures over the past two millenia. Geophys Res Lett 30:1820. https://doi.org/10.1029/2003GL017814
Maxbauer DP, Feinberg JM, Fox DL (2016) MAX UnMix: a web application for unmixing magnetic coercivity distributions. Comput Geosci 95:140–145
Mazari RK, Bagati TN, Chauhan MS, Rajagopalan G (1995) Palaeoclimatic record of last 2000 years in Trans-Himalayan Lahaul-Spiti Region. In: Proceedings of Nagoya IGBP-PAGES/PEP-II symposium, pp 262–269
Minyuk PS, Borkhodoev VY, Wennrich V (2014) Inorganic geochemistry data from Lake El'gygytgyn sediments: marine isotope stages 6–11. Clim past 10:467–485
Mishra PK, Anoop A, Schettler G, Prasad S, Jehangir A, Menzel P, Naumann R, Yousuf AR, Basavaiah N, Deenadayalan K, Wiesner MG (2015a) Reconstructed late quaternary hydrological changes from Lake Tso Moriri, NW Himalaya. Quat Int 371:76–86
Mishra PK, Prasad S, Anoop A, Plessen B, Jehangir A, Gaye B, Menzel P, Weise SM, Yousuf AR (2015b) Carbonate isotopes from high altitude Tso Moriri Lake (NW Himalayas) provide clues to late glacial and Holocene moisture source and atmospheric circulation changes. Palaeogeogr Palaeoclimatol Palaeoecol 425:76–83
Mishra PK, Prasad S, Marwan N, Anoop A, Krishnan R, Gaye B, Basavaiah N, Stebich M, Menzel P, Riedel N (2018) Contrasting pattern of hydrological changes during the past two millennia from central and northern India: regional climate difference or anthropogenic impact? Glob Planet Change 161:97–107
Misra P, Tandon SK, Sinha R (2019) Holocene climate records from lake sediments in India: assessment of coherence across climate zones. Earth Sci Rev 190:370–397
Nesbitt HW, Markovics G (1997) Weathering of granodioritic crust, long-term storage of elements in weathering profiles, and petrogenesis of siliciclastic sediments. Geochim Cosmochim Acta 61:1653–1670
Nesbitt H, Young GM (1982) Early Proterozoic climates and plate motions inferred from major element chemistry of lutites. Nature 299:715–717
Nesbitt HW, Markovics G, Price RC (1980) Chemical processes affecting alkalis and alkaline earths during continental weathering. Geochim Cosmochim Acta 44:1659–1666
Owen LA, Benn DI, Derbyshire E, Evans DJA, Mitchell WA, Richardson S (1996) The Quaternary glacial history of the Lahul Himalaya, Northern India. J Quat Sci 11:25–42
Owen LA, Gualtieri L, Finkel RC, Caffee MW, Benn DI, Sharma MC (2001) Cosmogenic radionuclide dating of glacial landforms in the Lahul Himalaya, northern India: defining the timing of Late Quaternary glaciations. J Quat Sci 16:555–563
Parcha SK, Pandey S (2016) Trace fossils and microbially induced sedimentary structures from the early Cambrian successions of

the Chandratal area, Spiti Basin, Tethys Himalaya. J Palaeontol Soc India 61:9–18
Peters C, Dekkers MJ (2003) Selected room temperature magnetic parameters as a function of mineralogy, concentration and grain size. Phys Chem Earth A/b/c 28:659–667
Petterson G, Renberg I, Geladi P, Lindberg A, Lindgren F (1993) Spatial uniformity of sediment accumulation in varved lake sediments in northern Sweden. J Paleolimnol 9:195–208
Phadtare NR (2000) Sharp decrease in summer monsoon strength 4000–3500 cal yr BP in the Central Higher Himalaya of India based on pollen evidence from alpine peat. Quat Res 53:122–129
Phartiyal B, Singh R, Joshi P, Nag D (2020) Late-Holocene climatic record from a glacial lake in Ladakh range, Trans-Himalaya, India. Holocene 30:1029–1042
Phartiyal B, Singh R, Nag D, Sharma A, Agnihotri R, Prasad V, Yao T, Karthick B, Joshi P, Gahlaud SK, Thakur B (2021) Reconstructing climate variability during the last four millennia from trans-Himalaya (Ladakh-Karakoram, India) using multiple proxies. Palaeogeogr Palaeoclimatol Palaeoecol. https://doi.org/10.1016/j.palaeo.2020.110142
Pokharia AK, Agnihotri R, Sharma S, Bajpai S, Nath J, Kumaran RN, Negi BC (2017) Altered cropping pattern and cultural continuation with declined prosperity following abrupt and extreme arid event at~ 4,200 yrs BP: Evidence from an Indus archaeological site Khirsara, Gujarat, western India. PLoS ONE. https://doi.org/10.1371/journal.pone.0185684
Pokharia AK, Kharakwal JS, Sharma S, Spate M, Tripathi D, Dimri AP, Liu X, Thakur B, Basumatary SK, Srivastava A, Mahar KS (2020) Variable monsoons and human adaptations: archaeological and palaeoenvironmental records during the last 1400 years in north-western India. Holocene 30:1332–1344
Prasad S, Anoop A, Riedel N, Sarkar S, Menzel P, Basavaiah N, Krishnan R, Fuller D, Plessen B, Gaye B, Röhl U (2014) Prolonged monsoon droughts and links to Indo-Pacific warm pool: a Holocene record from Lonar Lake, central India. Earth Planet Sci Lett 391:171–182
Prasad S, Marwan N, Eroglu D, Goswami B, Mishra PK, Gaye B, Anoop A, Basavaiah N, Stebich M, Jehangir A (2020) Holocene climate forcings and lacustrine regime shifts in the Indian summer monsoon realm. Earth Surf Proc Land 45:3842–3853
Quamar MF (2019) Vegetation dynamics in response to climate change from the wetlands of Western Himalaya, India: Holocene Indian summer monsoon variability. Holocene 29:345–362
Rawat S, Phadtare NR, Sangode SJ (2012) The Younger Dryas cold event in NW Himalaya based on pollen record from the lake sediments in Himachal Pradesh, India. Curr Sci 102:1193–1198
Rawat S, Gupta AK, Sangode SJ, Srivastava P, Nainwal HC (2015a) Late Pleistocene-Holocene vegetation and Indian summer monsoon record from the Lahaul, Northwest Himalaya, India. Quat Sci Rev 114:167–181
Rawat S, Gupta AK, Srivastava P, Sangode SJ, Nainwal HC (2015b) A 13,000 year record of environmental magnetic variations in the lake and peat deposits from the Chandra valley, Lahaul: implications to Holocene monsoonal variability in the NW Himalaya. Palaeogeogr Palaeoclimatol Palaeoecol 440:116–127
Rawat V, Rawat S, Srivastava P, Negi PS, Prakasam M, Kotlia BS (2021a) Middle Holocene Indian summer monsoon variability and its impact on cultural changes in the Indian subcontinent. Quat Sci Rev 255:106825. https://doi.org/10.1016/j.quascirev.2021.106825
Rawat V, Rawat S, Srivastava P, Negi PS, Prakasam M, Kotlia BS (2021b) Multiproxy paleoclimate dataset from the Bednikund alpine lake in the Central Himalaya. Data Brief 35:106930. https://doi.org/10.1016/j.dib.2021.106930
Reimer PJ, Bard E, Bayliss A, Beck JW, Blackwel PG, Bronk Ramsey C, Buck CE, Cheng H, Edwards RL, Friedrich M, Grootes PM (2013) IntCal13 and Marine13 radiocarbon age calibration curves 0–50,000 years cal BP. Radiocarbon 55:1869–1887
Roberts AP, Cui Y, Verosub KL (1995) Wasp-waisted hysteresis loops: mineral magnetic characteristics and discrimination of components in mixed magnetic systems. J Geophys Res Solid Earth 100:17909–17924
Rowan AV (2017) The 'Little Ice Age' in the Himalaya: a review of glacier advance driven by Northern Hemisphere temperature change. Holocene 27:292–308
Rühland K, Phadtare NR, Pant RK, Sangode SJ, Smol JP (2006) Accelerated melting of Himalayan snow and ice triggers pronounced changes in a valley peatland from northern India. Geophys Res Lett 33:L15709. https://doi.org/10.1029/2006GL026704
Saha S, Owen LA, Orr EN, Caffee MW (2018) Timing and nature of Holocene glacier advances at the northwestern end of the Himalayan-Tibetan orogen. Quat Sci Rev 187:177–202
Sarkar S, Wilkes H, Prasad S, Brauer A, Riedel N, Stebich M, Basavaiah N, Sachse D (2014) Spatial heterogeneity in lipid biomarker distributions in the catchment and sediments of a crater lake in central India. Org Geochem 66:125–136
Schiefer E (2006) Depositional regimes and areal continuity of sedimentation in a montane lake basin, British Columbia, Canada. J Paleolimnol 35:617–628
Shah RA, Achyuthan H, Lone AM, Kumar S, Kumar P, Sharma R, Amir M, Singh AK, Dash C (2020) Holocene palaeoenvironmental records from the high-altitude Wular Lake, Western Himalayas. Holocene 30:733–743
Shamurailatpam MS, Kumar O, Ramanathan AL (2020) Testing the reliable proxies to understand the mid-Holocene climate variability records from Chandratal lake, Western Himalayas. Quat Int. https://doi.org/10.1016/j.quaint.2020.11.003
Sharma S, Joachimski M, Sharma M, Tobschall HJ, Singh IB, Sharma C, Chauhan MS, Morgenroth G (2004) Lateglacial and Holocene environmental changes in Ganga plain, Northern India. Quat Sci Rev 23:145–159
Sharma A, Kumar K, Laskar A, Singh SK, Mehta P (2017) Oxygen, deuterium, and strontium isotope characteristics of the Indus River water system. Geomorphology 284:5–16
Shekhar M, Bhardwaj A, Singh S, Ranhotra PS, Bhattacharyya A, Pal AK, Roy I, Martín-Torres FJ, Zorzano MP (2017) Himalayan glaciers experienced significant mass loss during later phases of little ice age. Sci Rep 7:10305. https://doi.org/10.1038/s41598-017-09212-2
Singh S, Gupta AK, Rawat S, Bhaumik AK, Kumar P, Rai SK (2021) Paleomonsoonal shifts during 13700 to 3100 yr BP in the central Ganga Basin, India with a severe arid phase at 4.2 ka. Quat Int. https://doi.org/10.1016/j.quaint.2021.01.015
Srikantia SV, Bhargava ON (2018) Stratigraphic nomenclature of early Palaeozoics of the Spiti Himalaya: Cobweb cleared. J Paleontol Soc India 63:233–241
Srivastava P, Agnihotri R, Sharma D, Meena N, Sundriyal YP, Saxena A, Bhushan R, Sawlani R, Banerji US, Sharma C, Bisht P (2017a) 8000-year monsoonal record from Himalaya revealing reinforcement of tropical and global climate systems since mid-Holocene. Sci Rep 7:14515. https://doi.org/10.1038/s41598-017-15143-9
Srivastava P, Kumar A, Chaudhary S, Meena N, Sundriyal YP, Rawat S, Rana N, Perumal RJ, Bisht P, Sharma D, Agnihotri R (2017b) Paleofloods records in Himalaya. Geomorphology 284:17–30
Srivastava P, Siddaiah NS, Sangode SJ, Meshram DC (2018a) Trace element behavior in moderately weathered boles from the Deccan volcanic province: implications for paleoenvironment. CATENA 169:151–163
Srivastava P, Siddaiah NS, Sangode SJ, Meshram DC (2018b) Mineralogy and geochemistry of various colored boles from the Deccan

volcanic province: implications for paleoweathering and paleoenvironmental conditions. CATENA 167:44–59

Srivastava P, Kumar A, Singh R, Deepak O, Kumar AM, Ray Y, Jayangondaperumal R, Phartiyal B, Chahal P, Sharma P, Ghosh R (2020) Rapid lake level fall in Pangong Tso (lake) in Ladakh, NW Himalaya: a response of late Holocene aridity. Curr Sci 119:219–231

Staubwasser M, Sirocko F, Grootes PM, Segl M (2003) Climate change at the 4.2 ka BP termination of the Indus valley civilization and Holocene south Asian monsoon variability. Geophys Res Lett 30:1425. https://doi.org/10.1029/2002GL016822

Steinhilber F, Beer J, Fröhlich C (2009) Total solar irradiance during the Holocene. Geophys Res Lett. https://doi.org/10.1029/2009GL040142

Wang J, Zhu L, Nishimura M, Nakamura T, Ju J, Xie M, Takahiro W, Testsuya M (2009) Spatial variability and correlation of environmental proxies during the past 18,000 years among multiple cores from Lake Pumoyum Co, Tibet, China. J Paleolimnol 42:303–315

Wang Y, Shen J, Wang Y, Liu X, Cao X, Herzschuh U (2020) Abrupt mid-Holocene decline in the Indian Summer Monsoon caused by tropical Indian Ocean cooling. Clim Dyn 55:1961–1977

Williamson D, Jelinowska A, Kissel C, Tucholka P, Gibert E, Gasse F, Massault M, Taieb M, Van Campo E, Wieckowski K (1998) Mineral-magnetic proxies of erosion/oxidation cycles in tropical maar-lake sediments (Lake Tritrivakely, Madagascar): paleoenvironmental implications. Earth Planet Sci Lett 155:205–219

Wünnemann B, Demske D, Tarasov P, Kotlia BS, Reinhardt C, Bloemendal J, Diekmann B, Hartmann K, Krois J, Riedel F, Arya N (2010) Hydrological evolution during the last 15 kyr in the Tso Kar lake basin (Ladakh, India), derived from geomorphological, sedimentological and palynological records. Quat Sci Rev 29:1138–1155

Zhisheng A, Clemens SC, Shen J, Qiang X, Jin Z, Sun Y, Prell WL, Luo J, Wang S, Xu H, Cai Y, Zhou W, Liu X, Liu W, Shi Z, Yan L, Xiao X, Chang H, Wu F, Ai L, Lu F (2011) Glacial-interglacial Indian summer monsoon dynamics. Science 333:719–723